Charles University

Faculty of Science

Study programme: Chemistry

Branch of study: Analytical chemistry

Bc. Veronika Garbárová

Novel fluorosensors based on naphthalimide derivatives
Nové fluorosenzory na bázi derivátů naftalimidu

Diploma thesis

Supervisor: doc. RNDr. Juraj Dian, CSc.

Prague, 2019

Prohlášení:

Prohlašuji, že jsem závěrečnou práci zpracovala samostatně a že jsem uvedla všechny použité informační zdroje a literaturu. Tato práce ani její podstatná část nebyla předložena k získání jiného nebo stejného akademického titulu.

V Praze, 17.05.2019

Podpis

Abstrakt

Cílem diplomové práce bylo připravit a charakterizovat fluorescenční senzory založené na fluoroforech a supramolekulárních systémech (cyklodextrinech) připojených k pevným nosičům.

V této práci byly jako pevné nosiče použity 75 μm skleněné kuličky s vhodnou derivatizací povrchu a dva typy nafionových membrán. Byly syntetizovány deriváty naftalimidu s kladně nabitou částí umožňující navázání na povrchy.

Kladně nabitý derivát naftalimidu byl nejdříve připojen elektrostatickými interakcemi na záporně nabité pevné nosiče a stupeň navazování byl sledován pomocí UV-VIS absorpční spektroskopie. Alternativně byl na pevný povrch rovněž navázán kladně nabitý derivát β-cyklodextrinu v ekvimolárním poměru s naftalimidovým fluoroforem.

Těžištěm práce bylo měření fluorescenční senzorové odezvy připravených systémů v plynné a kapalné fázi na homologickou řadu n-alkoholů (methanol až n-hexanol). Pro studované senzorové systémy byly vyhodnoceny vybrané statické a dynamické senzorové parametry – citlivost, mez detekce, lineární dynamický rozsah a časová konstanta senzorové odezvy.

Praktická využitelnost připravených senzorových systémů byla zkoumána pro detekci ethanolu v benzínu. Měření fluorescenční senzorové odezvy senzorových systémů na bázi naftalimidového fluoroforu a β-cyklodextrinů připojených k nafionové membráně potvrzují realizovatelnost navrženého senzorového systému.

Klíčová slova: fluorescence, fluorofor, pevná fáze, chemosenzor, plynový senzor

Abstract

The aim of the diploma thesis was to prepare and characterize fluorescence sensor systems based on fluorophores and supramolecular components – cyclodextrins - attached to solid supports.

In this work, functionalized 75 μm glass beads and two types of Nafion membranes were used as negatively charged solid surfaces. Derivatives of naphthalimide with a positively charged part allowing the attachment to surfaces were synthesized.

The positively charged naphthalimide derivative was then attached on negatively charged surfaces via electrostatic interactions and the binding to the solid supports was examined using UV-VIS spectroscopy. Alternatively, the positively charged β-cyclodextrin derivative was also attached to the surface in an equimolar ratio with PNI-HEMPDA.

The focus of the work were measurements of fluorescence sensor responses in the gas and liquid phase to linear alcohols – methanol to n-hexanol – for all sensor systems. For the studied sensor systems, the selected sensor parameters were determined – sensitivity, the limit of detection, linear dynamic range and a sensor response time constant.

A practical application of the novel sensor system for the detection of ethanol in gasoline was examined. Fluorescence sensor response measurements of the prepared systems based on naphthalimide and β-cyclodextrin derivatives attached on Nafion membrane confirm the feasibility of the proposed sensor system.

Keywords: fluorescence, fluorophore, solid surface, chemosensor, gas sensor

Acknowledgment

I would like to thank Assoc. prof. Juraj Dian, Ph.D. for the professional supervising of this diploma thesis.

I would also like to thank consultants, Assoc. prof. Ivan Jelínek, Ph.D. and Assoc. prof. Jindřich Jindřich, Ph.D., for valuable advice regarding the thesis.

I am grateful to my parents for all the support.

Table of contents

List of symbols and abbreviations

CD	cyclodextrin
DNS	dansyl
ESIPT	excited state intramolecular proton transfer
EW	equivalent weight
FRET	fluorescence resonance energy transfer
HEMPDA	N^1,N^1,N^1,N^3,N^3,N^3,2-heptametyl-2-((prop-2-in-1--yloxy)methyl)propane-1,3-diaminium
ICT	intramolecular charge transfer
IEC	ion exchange capacity
LOD	limit of detection
Nafion	Nafion® - registered trademark of DuPont™
PEM	proton-exchange membrane, also referred to as polymeric electrolyte membrane
PET	photo-induced electron transfer
PFSI	perfluorosulfonate ionomer
PFSA	perfluorosulfonic acid
PNI	*N*-propyl-1,8-naphthalimide
PTFE	polytetrafluoroethylene
TEEG	tetraethyleneglycol
UV	ultraviolet
VIS	visible

1 INTRODUCTION

The development of automated systems for the detection of chemical substances represents one of the primary research directions in modern analytical chemistry. Optical fluorescence sensors and sensor arrays are very promising for this application due to their sensitivity, selectivity and response rate. A key component of these devices, which directly determines their sensor response characteristics, is a sufficiently stable chemically sensitive layer with a bonded fluorescent dye.

The design and optimization of the chemical modification of solid surfaces with fluorescent dyes is, therefore, a crucial step in the further development of new types of optical fluorescence sensors for sensitive and selective detection of selected analytes.

This research aims at preparation and characterization of fluorescence sensor systems based on naphthalimide fluorophores attached to solid supports. Optically transparent and easy to modify glass surface seems to be proper support. Another choice of appropriate support is a Nafion membrane - a sulfonated tetrafluoroethylene-based fluoropolymer-copolymer.

The modifications of solid surfaces and binding of fluorophores are one of the critical steps for the preparation of targeted sensor materials with desirable operational characteristics. Measurements of fluorescence sensor responses to the selected analytes in gas and liquid phase enable to determine operational sensor parameters of the newly prepared systems. Simultaneous attachment of a fluorophore and cyclodextrin on solid support enables to induce a molecular recognition process and improve the selectivity of sensor response.

2 THEORETICAL PART

2.1 Photoluminescence

2.1.1 Fluorescence and phosphorescence

Photoluminescence is the emission of light from excited electronic states when excitation occurred via photon absorption and depends on the nature of the excited state, Photoluminescence of organic molecules is divided into two categories — fluorescence and phosphorescence.

When the molecule absorbs the energy of an appropriate wavelength, one of the pair electrons of molecular orbital can get to the first excited singlet state S_1. If S_1 is relatively stable, the molecule can get via non-radiant transition to the lowest vibrational state of the excited state S_1. Consequently, photon emission in UV or VIS spectrum can occur, when the electron returns to the ground state S_o (Fig. 1)

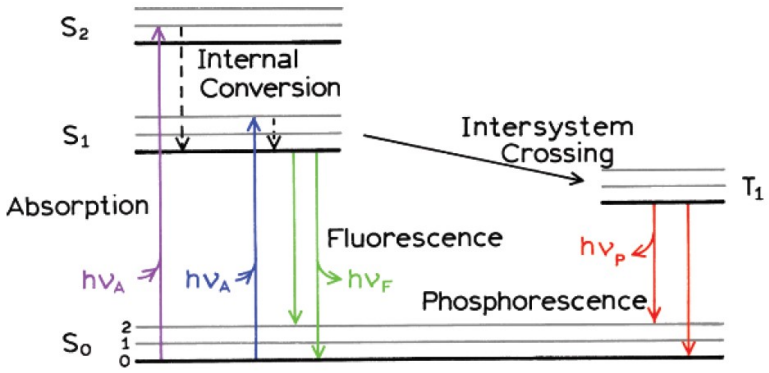

Fig. 1: Jablonski diagram – fluorescence and phosphorescence [2]

The emission rates of fluorescence are typically 10^8 s^{-1} and a fluorescence lifetime is of the order of 1 to 10 ns. The energy of the emission is typically less than the energy of the absorption, so fluorescence occurs at longer wavelengths.

In another case, if there is a mechanism for unpairing two electron spins, the molecule may undergo intersystem crossing - a nonradiative transition between states of different multiplicity - and get to the excited triplet state T_1. Now the transition from T_1 to the S_0 is forbidden. Therefore, the emission rates are much slower (10^3 to 10^0 s^{-1}) and phosphorescence lifetimes are typically milliseconds to seconds[3].

2.1.2 Fluorescence lifetime and quantum yield

The fluorescence lifetime τ and quantum yield η are the essential characteristics of a spectral transition of a fluorophore.

The fluorescence quantum yield is the ratio of the number of photons emitted (N_{emit}) to the number absorbed (N_{abs}), and it is expressed as:

$$\eta = \frac{N_{emit}}{N_{abs}} \quad (2.1.1)$$

Another way to define the quantum yield of fluorescence is by the rate of excited state decay:

$$\eta = \frac{k_r}{k_r + k_{nr}} \quad (2.1.2)$$

where η is the quantum yield, k_r is the emissive rate of the fluorophore and k_{nr} is rate of the non-radiative decay (Fig. 2).

The lifetime of the excited state (τ) is defined by the average time the molecule spends in the excited state before return to the ground state, and it is given by:

$$\tau = \frac{1}{k_r + k_{nr}} \quad (2.1.3)$$

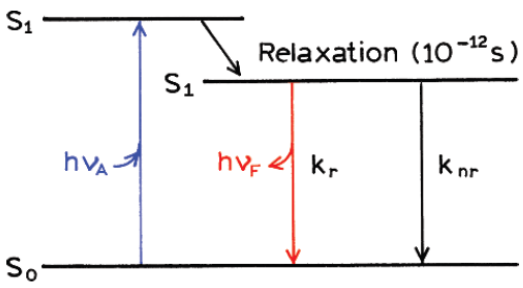

Fig. 2: Jablonski diagram illustrating quantum yield and fluorescence lifetime, k_r means the emissive rate of the fluorophore and k_{nr} is rate the of the non-radiative decay[2].

2.1.3 Fluorescence quenching

Fluorescence quenching includes various processes of non-radiative decays of the excited-state and can proceed via different mechanisms.

Collisional quenching occurs, when the excited-state of a fluorophore is deactivated upon contact with a quencher - another molecule, e.g., oxygen, halogens, amines, or electron-deficient molecules (Fig. 3 - k_q is the bimolecular quenching constant, [Q] is the quencher concentration)[2].

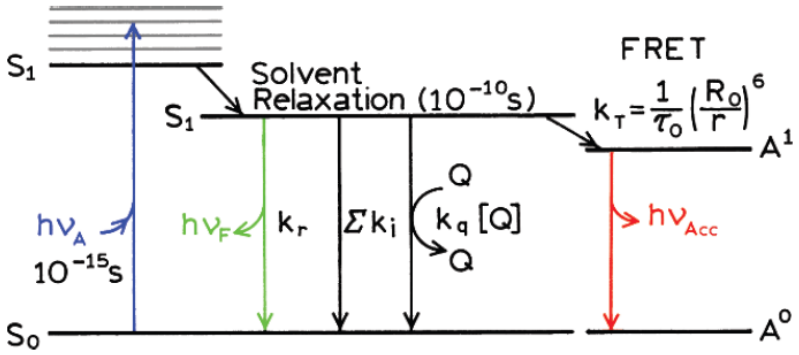

Fig. 3: Jablonski diagram showing fluorescence quenching. The term Σk_i means the sum of rate constants of all non-radiative paths to the ground state aside from quenching.[2]

Static quenching happens when fluorophores form non-fluorescent complexes with quenchers. Fluorescence can also be quenched via non-molecular mechanisms, such as attenuation of the fluorescence emission by the fluorophore itself or other absorbing species[2].

Fluorescence resonance energy transfer (FRET) is another important non-radiative process of the excited state deactivation (Fig. 3). This process transfers energy from one fluorophore molecule, called the donor, to the other molecule, called the acceptor, provided there is sufficient overlap between their optical spectra. The donor and acceptor need to be connected by a dipole-dipole interaction[4].

2.2 Sensors

2.2.1 Definition and classification

The sensor is "a device which provides a usable *Output* in response to a specified *Measurand*" as defined by ISA (Instrument Society of America)[5].
One of the many other definitions of chemical sensors mentions that they are miniaturized devices which convert a chemical state into an electrical signal. A chemical state is determined by the different concentrations, partial pressures, or activities of atoms, molecules, ions, or compounds, to be detected in the gas, liquid, or solid phase[6].

Sensors can be classified by various criteria[7]:

- measured quantity – concentration, pressure, temperature, etc.
- physical or chemical effect (transduction principle) – optical, chemical and biochemical, mechanical, electrical, magnetic, radiant, thermal.
- technology, material and cost
- application and accuracy

Detailed classifications have been reported[8], but preferences for any of these criteria generally depend on the user.

2.2.2 The sensor´s properties

Sensor´s parameters can be divided into static and dynamic.

The most important static parameters are the following:

1. *Sensitivity* (the slope of the calibration curve) is defined as a ratio of the output (y) to the input (x):

$$S = \frac{\Delta y}{\Delta x}, \tag{2.2.2}$$

where Δy is the desired measurand and Δx is the output – e.g. change of concentration.

2. *Specificity* expressed the ability of the sensor to detect only the desired compound. However, it is complicated to realize in practice, and the sensor´s requirements are depending on the usage.
3. *Reliability,* which is expressed by:
    - *Accuracy* - the closeness of agreement between a measured quantity value (sensor output) and a true quantity value of a measurand[9]
    - *Precision* - the closeness of agreement between measured quantity values obtained by replicate measurements on the same or similar objects under specified conditions[9]
    - *Repeatability* - measurement precision under a set of repeatability conditions of measurement[9]
    - *Reproducibility* - the condition of measurement, out of a set of conditions that includes different locations, operators, measuring systems, and replicate measurements on the same or similar objects[9]
    - *Stability* - the period during which the device maintains repeatable and reproducible results
    - *Robustness* – the endurance of key parameters to small changes in experimental conditions
4. *Noise* is a part of the signal that carries no direct information. The noise is due to either internal noise sources, such as resistors at finite temperatures, or externally generated mechanical and electromagnetic fluctuations.

5. *Limit of detection* – the lowest concentration which can be qualitatively determined and is usually expressed as double of the standard deviation of the noise.
6. *Dynamic range* is the interval, in which the change of concentration causes a change in the sensor´s signal output. *The linear dynamic range* is an interval in which the change is linear.

Dynamic parameters describe the sensor response to a variable input which is different from that exhibited when the input signals are constant. They include a time constant *t*, the width of the spectral interval transfer function, frequency response, impulse response, and step response[6].

2.2.3 Optical chemosensors

The ideal chemical sensor is a device that can be inserted into a sample and will display the result of the chemical analysis in real time with excellent precision and selectivity. There are increasing interest and continuous improvement in the development of such sensors as they are still rare at present.

The optical chemosensor can offer the following advantages in comparison to other chemical sensor types: they do not need a reference element, they are easily miniaturized, the coupling of optodes allows the simultaneous monitoring of various analytes, they enable remote sensing, the performance of analysis in almost real time, no sampling is necessary.

On the other hand, the disadvantages are that additional instruments are needed for signal processing, the ambient light interferes, some optodes have limited long-term stability or dynamic ranges and that more specific sensors still have to be found[6].

Depending on the origin of the signal, the devices are classified as absorbance, reflectance, fluorescence, phosphorescence, Raman, light scattering, refractive index, or chemiluminescence sensors.

Optical sensors can be used for remote spectrometry, process control, pollution monitoring, biomedical sensing, and many others[10].

2.3 Fluorosensors

The development of fluorescent molecular systems for chemical recognition has recently received growing attention, based on their high selectivity, reasonable sensitivity, short response time, nondestructive methodology, direct visual perception and operational simplicity [11]. An advantage of fluorescence spectroscopy is that different assays can be designed based on changes in experimental parameters of the fluorescence output (intensity, lifetime, polarization anisotropy). Fluorescence does not consume analytes, and no reference is required. The fiber optics and detection technologies are well established and make possible to perform remote monitoring. Moreover, there are sensitive techniques that allow even the detection of single molecules[12].

Therefore, a very high level of sophistication and performance in terms of sensitivity, selectivity, and versatility is the reason that fluorosensors can be expected to be the most crucial future detection method.

2.3.1 Principle and design of fluorosensors

The classical construction of a fluorescent chemosensor usually includes two integrated components: a receptor responsible for the molecular recognition of the analyte and a fluorophore responsible for signalizing the recognition event. When a guest species is bound to the receptor, the photophysical characteristics of the fluorophore, such as fluorescence intensity, emission wavelength and fluorescence lifetime, will change and provide a signal that indicates guest binding[13]. The signal can be changed via different mechanism: photo-induced electron transfer (PET), charge transfer, FRET, or simple microenvironment changes[14].

PET-based sensors are composed of a "fluorophore–spacer–receptor" system (Fig. 4). After excitation of the fluorophore, electron transfer to the receptor part results in the exclusion of the fluorescence process. When a molecule of the analyte interacts with the receptor site, the PET process is stopped, and excitation of the fluorophore results in the emission of photons under the form of fluorescence[15].

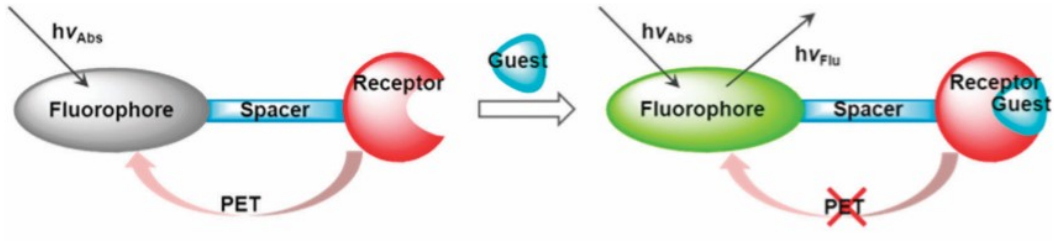

Fig. 4: The general demonstration of the principle of PET sensors [16].

In intramolecular (also called internal) charge transfer (ICT) sensors, the fluorophore and the receptor are directly connected (Fig. 5). They are based on "donor–fluorophore-acceptor" construction. The binding a guest analyte at either the electron donor or acceptor regions causes an alternation in the dipole strength of electron donor-acceptor pair and thus changes in intensities and spectral shifts[17].

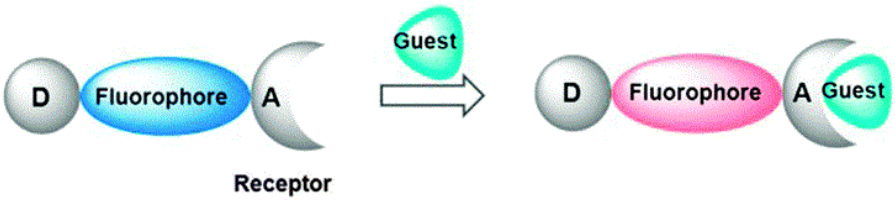

Fig. 5: The illustration of the principle of ICT sensors[16].

A special class of fluorophores uses excited state intramolecular proton transfer (ESIPT) when there is the possibility of proton transfer between two sites of the molecule, typically in keto-enol tautomers. The difference between tautomers in the ground and the excited state leads to the transfer of a proton upon excitation, resulting in the shift in the wavelength of emission[18].

2.3.2 Fluorophores

The development of new fluorophores based on organic molecules has gained interest in recent decades due to the progress in organic synthesis. The main objectives for the search of the new fluorophores are high fluorescence quantum yields, photochemical stability, structural controllability and binding to the solid surfaces, and biocompatibility[19].

2.3.2.1 Naphthalimide

Naphthalimide is a colorless compound which becomes colored by substitution with electron donating groups, preferably in 4- or 5-position by nitrogen or sulfur groups[20] (Fig. 6).

Fig. 6: 1,8-Naphthalimide derivative

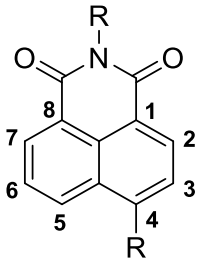

Naphthalimide is frequently used as a fluorophore because of its desirable characteristics, e.g., high photostability, significant Stokes shift, and high fluorescence quantum yield[21]. The 1,8-naphthalimide structure can undergo ICT process which has attracted considerable attention in recent years.

Naphthalimide dyes have acquired industrial importance; they are used as brilliant yellow dyes in synthetic fiber technology and as an optical brightener[22].

Fluorescent probes based on naphthalimide had wide applications in biology. They have been used for detection of glutathione in the lysosomes of living cells[23], were found to have cytotoxic activity[24], and used as fluorescent cellular imaging agents[25].

Naphthalimide-based systems capable of recognizing biologically relevant cations or anions have been reported, including efficient fluorescent probes for silver cation[21, 26] or sensor which exhibits a strong selectivity toward Hg^{2+}[27]. The selective sensor for recognition of Cr^{+3} and S^{2-} suitable for monitoring intracellular conditions[28], or system that could selectively recognize fluoride anions in the presence of other anions were described as well.[29, 30].

Recently, even a sensor for dual-mode sensing based on 1,8-naphthalimide coupled with a hydrazone linker containing a quinoline group that can detect and differentiate CN^- and F^- was developed[31].

The solvatochromic properties of naphthalimide – solvent polarity dependent absorption and fluorescence emission – were used to demonstrate the possibility to differentiate halogenated solvents using fluorescence sensor[32].

2.4 Cyclodextrins

2.4.1 Structure and properties

Cyclodextrins (CDs) are cyclic oligosaccharides obtained from enzymatic degradation of starch. The three most abundant CDs have six, seven or eight glucose units and they are named as α, β and γ-CD, respectively[33] (Fig. 7).

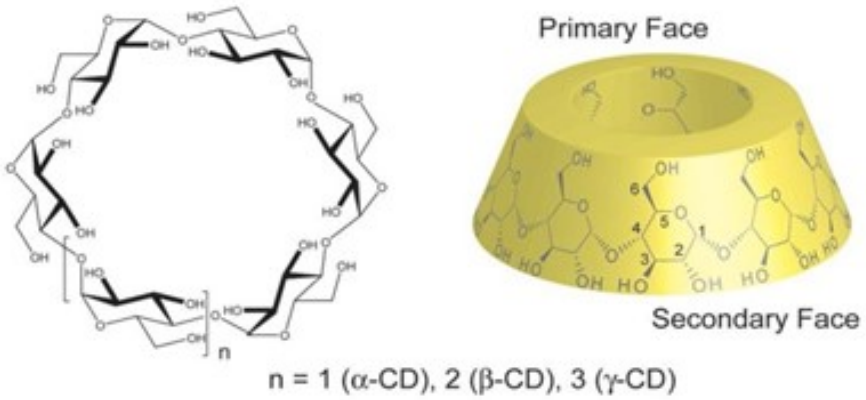

Fig. 7: Chemical structure (left) and 3D structure (right) of CDs[1].

CDs have a shape of a hollow truncated cone with the relatively hydrophobic inner cavity and a hydrophilic outer surface. (Fig. 6) This structure enables CD molecule to act as host for guest molecules, which can be incorporated into the cavity and thus formed supramolecular host-guest complexes, also known as inclusion complexes.[7] Inclusion complexes are formed due to non-covalent interactions, such as hydrogen bonding, hydrophobic, van der Waals and electrostatic interactions, and exclusion of cavity-bound high-energy water[8].

Tab. 1: Properties of α,β and γ-CD[1].

	α-CD	β-CD	γ-CD
Number of glucose units	6	7	8
Molecular Weight	972.86	1135.01	1297.15
Water Solubility (g/L)	145	18.5	232
Internal Diameter	4.7-5.2	6.0-6.4	7.5-8.3
Depth	6.7	7.0	7.0

Due to their unique structure, CDs have found applications in food industry[34, 35], cosmetics[36], pharmacy[37], analytical chemistry[38], biotechnology[39], sensors[40], and many others.

2.4.2 Molecular recognition of cyclodextrins

The inclusion of guest fluorescent molecules into the CD cavity can be detected because changes in the microenvironment of chromophores generally result in a change of their color and fluorescence properties[40].

Chromophore-modified CDs can be divided into two types: "turn-off" and "turn-on." In "turn-off" type, fluorophore-CD connected via a flexible linker form a self-inclusion complex and the fluorescence intensity is weakened by complexation with guest molecules (Fig. 8a). When a competitive guest is added, the fluorophore is excluded from the hydrophobic cavity to aqueous media, resulting in a decrease of its fluorescence intensity. Many kinds of "turn-off" fluorescent sensors were developed[41-43].

In "turn-on" fluorescent chemical sensors, the fluorescence intensity is increased by the formation of host-guest complexes (Fig. 8b). CD and fluorophore are connected with a rigid spacer and thus could not form self-inclusion complexes. When a hydrophobic guest molecule is included in the cavity of the CD, the fluorophore is located in a more hydrophobic environment, thus the fluorescence intensity increases[1]. Many sensors belonging to this new "turn-on" type were reported[44, 45].

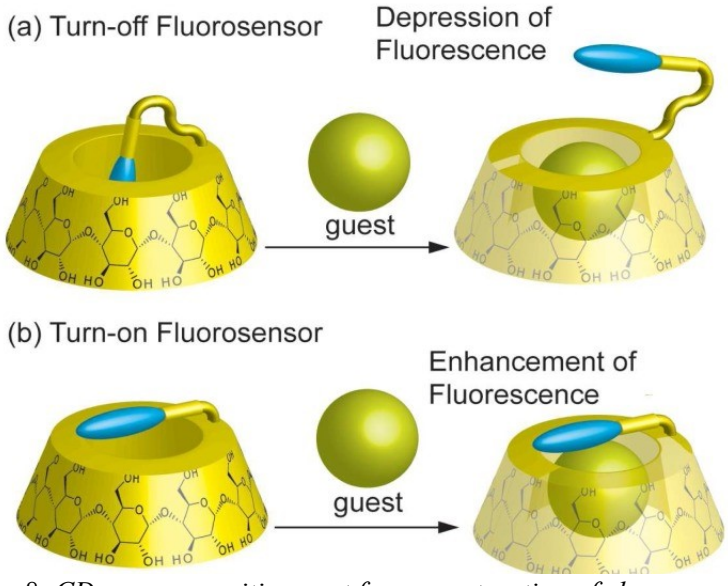

Fig. 8: CD as a recognition part for a construction of chemosensors.[1].

Another possibility of a chemical sensing is an approach when the binding site of CD and signalizing fluorophore are not covalently linked but form a supramolecular ensemble on a solid surface. The interaction between the receptor and detected host molecule causes replacement of the receptor in the cavity, which results in significant variations in the optical properties.

Supramolecular ensembles have advantages over conventional approaches as they are in thermodynamic equilibrium and kinetically reversible and therefore the reaction could proceed to the desired state of host-guest binding by controlling the conditions. Furthermore, complicated chemical syntheses of specific covalently bounded fluorophore-CD derivatives can be avoided[46].

2.5 Solid supports

After the production of a signalizing (transducer) and recognition part of the fluorescent sensor, the next step toward the fabrication of a chemosensor is usually the incorporation of the fluorophore to/into solid support[12]. The stable solid sensor material with attached fluorescence dye is crucial in the development of fluorosensors and has a direct influence on the sensor's characteristics.

In this work, the glass beads and Nafion membranes were chosen as representative solid surfaces with a different way of fluorophore binding to the solid state.

2.5.1 Glass beads

The glass possesses the following appropriate properties: it is optically transparent at wavelengths above 320 nm, it has low intrinsic fluorescence and easy surface functionalization[47]. A simple planar glass has the disadvantage of the small surface/volume ratio. Therefore, glass beads with narrow size dispersion have already been already used as supportive material for various applications due to their mechanical strength and low price[48]. Modified glass beads were applied in the production of polymers, pharmacy, agriculture, environmental science and other industrial processes[49].

2.5.2 Nafion membrane

Nafion perfluorosulfonic acid (PFSA) membranes are homogeneous, transparent and mechanically strong films based on a chemically stabilized copolymer of PFSA and polytetrafluoroethylene (PTFE) in the acid form. PTFE builds a hydrophobic backbone system in which are incorporated perfluoro vinyl ether groups terminated with hydrophilic sulfonate groups.

The resulting structure of the copolymer is shown in Fig. 9.

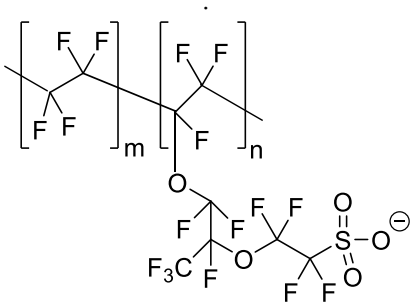

Fig. 9: Structure of the Nafion membrane

Fluorocarbon part of Nafion is resistant to chemical attacks while sulfonic acid groups enable Nafion function as an acid catalyst and ion exchange resin. Moreover, the sulfonic groups form ionic channels in the hydrophobic polymer, and water is very easily transported through them. Nafion can thus function as a permeable membrane to water and cations, while it is impermeable to anions[50].

2.5.2.1 Preparation of Nafion membranes

The preparation of Nafion starts with the copolymerization of tetrafluoroethylene and perfluoro vinyl ether. The resulting product is a sulfonyl fluoride ($–SO_2F$) form of perfluorosulfonate ionomer (PFSI) which can be melt-extruded into membranes. Hot aqueous NaOH converts $-SO_2F$ groups into sulfonate ($-SO_3^-Na^+$), which are finally converted to the acid form containing the sulfonic acid ($-SO_3H$) groups.

Thinner films can be obtained when the acidic form of PFSI is heated in alcoholic solvents in an autoclave and then tape-casted into membranes of required thickness[51].

Methods for preparation of the membranes are continually being improved, in order to increase the material stability, reduce the thickness and decrease the ionic resistance. However, as with all industrial processes, not all the details of the synthesis are available [52].

2.5.2.2 Nomenclature

Taken that molecular weight of Nafion is uncertain due to differences caused by the production and morphology, the equivalent weight (EW) and material thickness are used instead to describe the most commercially available membranes.

The EW is the number of grams of dry Nafion per mole of sulfonate groups when the material is in the acid form. Interchangeably, ion exchange capacity (IEC) is used, which is reciprocal of the equivalent weight, i.e., IEC = 1000/EW[53].

The thickness is expressed in the last digit in the name, which means multiple of a thousandth of an inch (25.4 µm).

Properties of the most used types of Nafion membranes are listed in (Tab. 2) [51].

Tab. 2: The commercial name, the thickness in inch resp. µm, EW and EIC for the most common Nafion membranes.

Name	Thickness / in	Thickness / µm	EW / ($g_{polymer}$/$mole_{SO_3H}$)	EIC / meq_{SO_3H}/$g_{polymer}$)
Nafion® N1100	0.010	254	1100	0.91
Nafion® N117	0.007	183	1100	0.91
Nafion® N115	0.005	127	1100	0.91
Nafion® NR-212	0.002	50.8	990 - 1050	0.95–1.01
Nafion® NR-211	0.001	25.4	990 - 1050	0.95–1.01

2.5.2.3 Applications of Nafion

Because of its unique properties, Nafion is used in a broad range of fields. It is widely used as Polymeric Electrolyte Membrane (PEM) for fuel cells[54], as a cell membrane for chlor-alkali production[55], or as a superacid catalyst in organic synthesis [56]. Nafion membranes also found applications in chemosensors, in the electrochemical solid-state gas sensor for carbon monoxide[57] or amperometric Pt–Nafion sensor for nitric oxide[58].

For application in optical chemosensors, derivatives of metallochromic indicator 1-(2'-pyridylazo)-2-naphthol (PAN) were immobilized in a Nafion membrane, and optode for the determination of Ni^{2+} [59] and a flow-through optical sensor for the determination of Cu^{2+} was prepared[60]. Luminescent ruthenium complex was immobilized in Nafion film as well, and new optical pH sensor was developed[61].

2.6 Determination of ethanol in fuels

Ethanol-blended gasoline is being introduced in many countries to assess emissions and energy consumption. While ethanol is considered a clean and renewable alternative fuel, it is used in blends with gasoline to increase oxygen content and thus decrease exhaust emissions of incomplete combustion products.
However, engines of older vehicles are not adapted to increasing ethanol percentages. As a result quantification of ethanol in blended gasoline becomes an important issue[62].

The American Society for Testing and Materials (ASTM) published a standard ASTM D5501 - 12(2016) which describes a standard test method for determination of ethanol and methanol content in fuels. However, this method is expensive, not easy to implement and requires the use of long columns (100 m and 150 m)[63].

Various methods have been described for measurement of ethanol concentration in gasoline fuels using different principles, specifically fluorescence spectroscopy, infrared spectroscopy[64], high-performance liquid chromatography[65], Raman spectroscopy[66], nuclear magnetic resonance spectroscopy[67], cyclic voltametry[68], amperometry[69], but developing of new methods is still a matter of interest.

3 EXPERIMENTAL PART

3.1 Materials

Nafion® 117 membranes were purchased from Ion Power, Inc (USA) and Nafion® 212 from Acros Organics. Glass beads with 75 μm diameter and (3-mercaptopropyl)trimethoxysilane, were purchased from Sigma Aldrich.
Analytes (methanol, ethanol, propanol, 1-butanol, 1-pentanol, 1-hexanol, toluene, benzene, hexane, dichloromethane, chloroform, aniline, phenol, nitrobenzene) were purchased from Lachema and dried before use with molecular sieves 4Å.

A derivative of fluorophore PNI-HEMPDA was synthesized according to a procedure described in my bachelor thesis[70]. Derivatives of cyclodextrins were synthesized at the Department of Organic chemistry, as a part of a project with the research group of doc. RNDr. Jindřich Jindřich, CSc., and synthesis of derivatives will be published.
Following derivatives were used in concentrations listed below:

- PNI-HEMPDA (M_r = 951.26 g mol^{-1}, c = 9.26·10^{-3} M)
- β-CD-TEEG-HEMPDA (M_r = 1868.53 g mol^{-1}, c = 9.32·10^{-5} M)
- γ-CD-TEEG-HEMPDA (M_r = 1992.59 g mol^{-1}, c = 9.03·10^{-5} M)

3.2 Preparation of samples

3.2.1 Preparation of sulfonated-glass beads

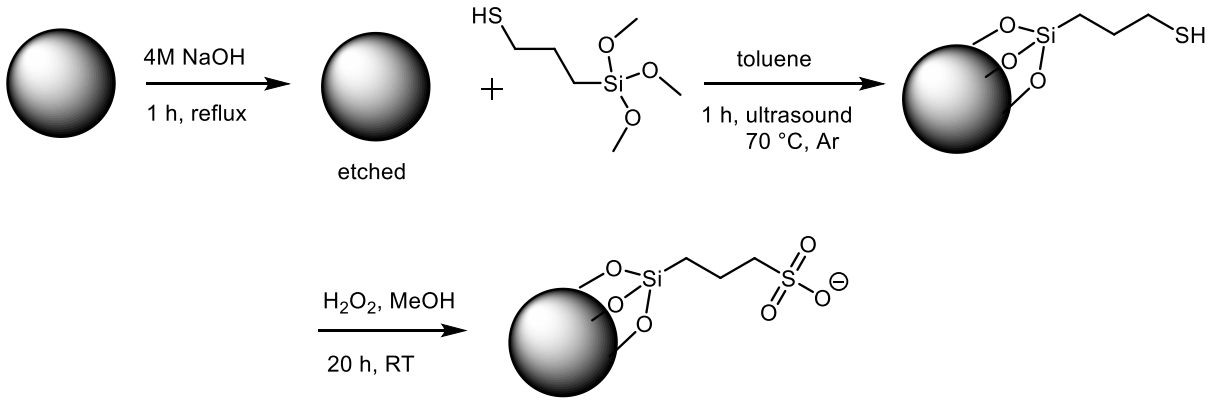

Scheme 1: Preparation of sulfonated-glass beads

The glass beads (5 g) were etched in 4 M NaOH solution (20 ml). The suspension was refluxed for 1 hour; the glass beads were filtered, washed with water to neutrality and dried under vacuum[71].

To the etched glass beads (5 g) was added (3-mercaptopropyl)trimethoxysilane (6.3 ml) and dry toluene (12.5 ml). The mixture was heated in ultrasound at 70 °C for 1 hour under argon. The glass beads were filtered, washed with acetone and dried under vacuum.

The silanized-glass beads (5 g) were oxidized with H_2O_2 (15 ml) in methanol (5 ml) for 24 hours at room temperature. Afterward, the glass beads were filtrated, washed with water, saturated $NaHCO_3$ solution, acetone and dried under vacuum.

3.2.2 Attachment of fluorophores to the surface of the sulfonated-glass beads

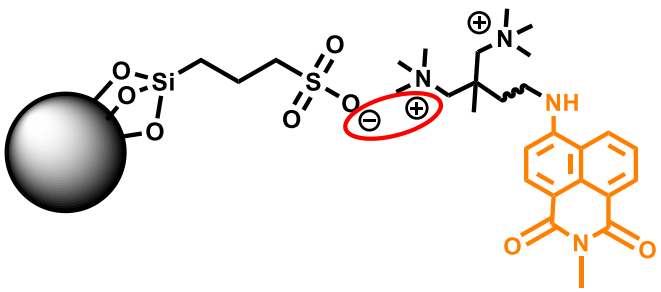

Scheme 2: Binding of PNI-HEMPDA on the surface of glass beads.

Sulfonated glass beads were functionalized with PNI-HEMPDA fluorophore via electrostatic attachment (Scheme 2).

Firstly, the dependence of the degree of fluorophore immobilization on glass beads surface as a function of reaction time was examined. To the solution of PNI-HEMPDA (2.5 ml; $9.25 \cdot 10^{-6}$ M) in a quartz cuvette, one dose of sulfonated-glass beads (100 mg) was added. Absorption spectra were measured after addition every 10 minutes up to 1 hour. No changes of absorption spectra in time were observed which suggests that immobilization on glass beads was completed immediately.

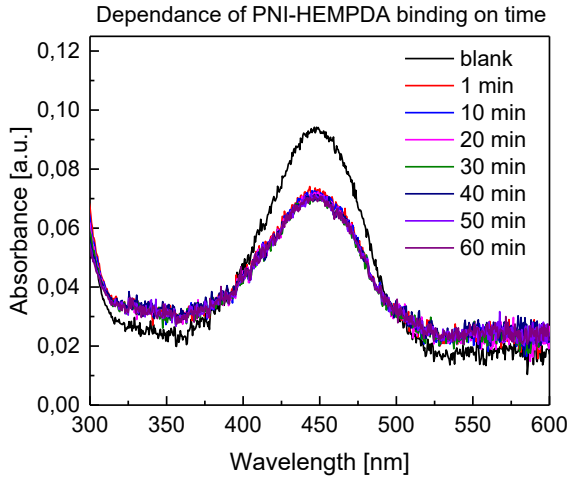

Fig. 10: Absorption spectra of the PNI-HEMPDA solution (2.5 ml; $9.25 \cdot 10^{-6}$ M) measured as a function of time after one addition of 100 mg dose of glass beads.

Then, the amount of PNI-HEMPDA bound to the surface of the glass beads was examined. Sulfonated-glass beads (100 mg) were subsequently added to the solution of

PNI-HEMPDA (2.5 ml; $1.85 \cdot 10^{-5}$ M) in a quartz cuvette. Absorption spectra were measured after every addition of 100 mg glass beads until PNI-HEMPDA was completely bounded (Fig. 11A). Values of absorbance at 450 nm were plotted against the mass of added glass beads. The calibration line obtained by linear fitting is in Fig. 11B:

$$A_{450} = 0.160 - 0.260 \cdot m_{GB}, \quad (3.2.1)$$

where A_{450} is the absorbance of PNI-HEMPDA at 450 nm and m_{GB} is the mass of added glass beads.

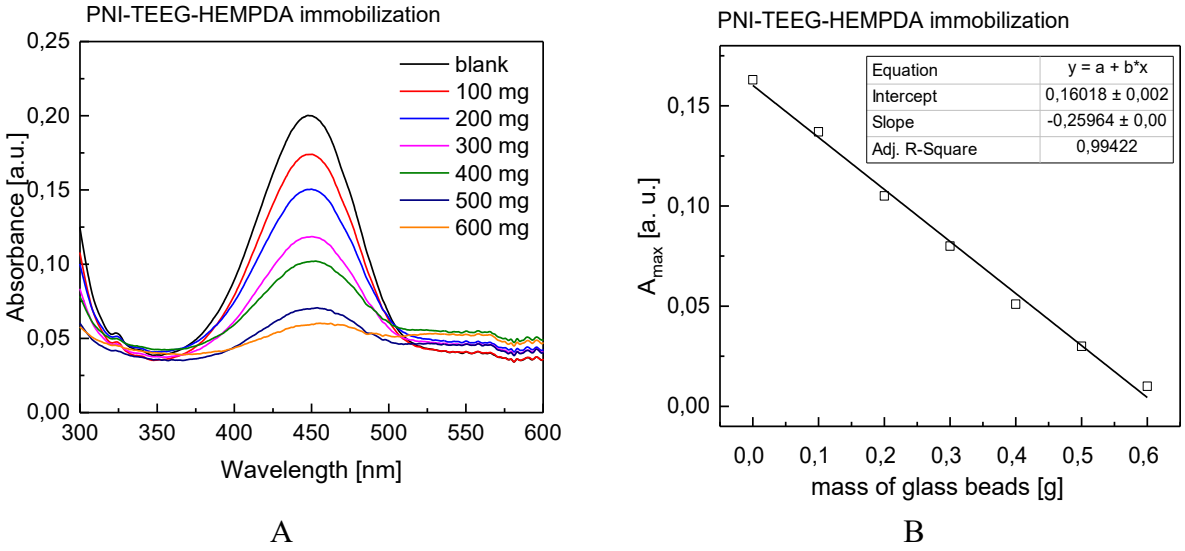

A B

Fig. 11: Absorption spectra measured after constant addition of glass beads (0.100 g) to the solution of PNI-HEMPDA (2.5 ml; $1.85 \cdot 10^{-5}$ M) (A), calibration line obtained by least-square fitting of the absorbance values at 450 nm against the mass of added glass beads (B).

As a next step, glass beads functionalized with both PNI-HEMPDA and CD derivatives were prepared according to the method described above. As follows from the calibration line (Fig. 11), $2.3 \cdot 10^{-8}$ mol of charged substance can be bounded on the surface of 200 mg glass beads. Therefore, equimolar solution (2.5 ml) of PNI-HEMPDA ($9.26 \cdot 10^{-6}$ M) and simultaneously either β-CD-TEEG-HEMPDA ($9.32 \cdot 10^{-6}$ M) or γ-CD-TEEG-HEMPDA ($9.03 \cdot 10^{-6}$ M) were added to sulfonated-glass beads (200 mg), and glass beads with attached fluorophore and CD were prepared.

3.2.3 Attachment of fluorophores on Nafion 117

The attachment of PNI-HEMPDA on the surface of Nafion via electrostatic interactions is schematically illustrated in Scheme 3:

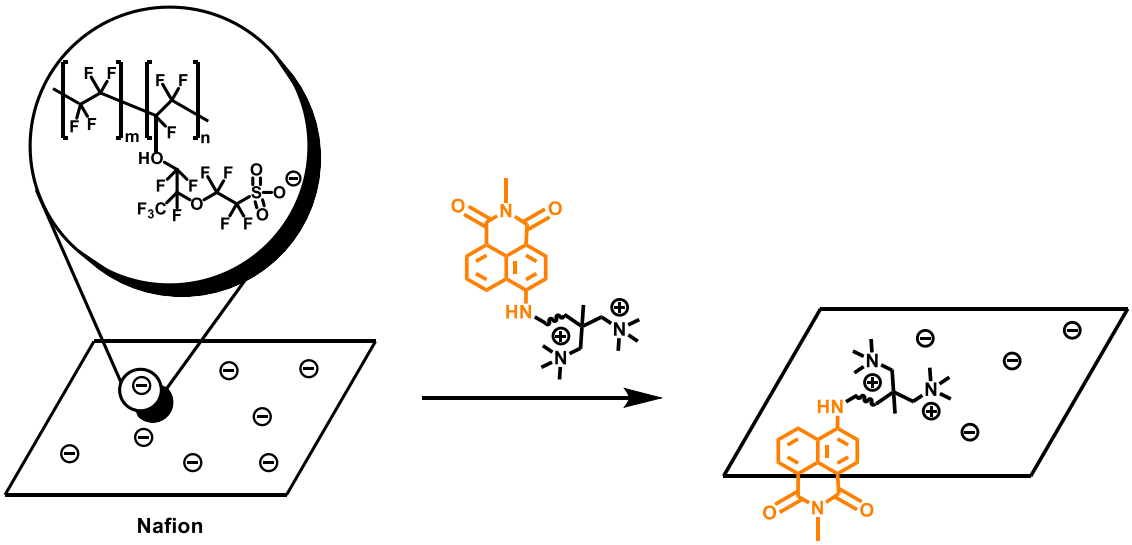

Scheme 3: Binding of PNI-HEMPDA to Nafion.

Nafion foil was immersed in a solution of PNI-HEMPDA ($1.0 \cdot 10^{-4}$ M, 3.0 ml) and absorption spectra of Nafion were measured as a function of time (Fig. 12A). Values of absorbance at 450 nm were plotted against time of binding, and experimental points were fitted with exponential dependence:

$$A(t) = A_0 \cdot \left(1 - e^{-\frac{t}{\tau}}\right), \tag{3.2.3}$$

where $A(t)$ is absorbance at 450 nm in time t, A_0 is absorbance at $t = 0$, and τ is a time constant. The value of τ for the binding of PNI-HEMPDA to Nafion was 56.7 min (Fig. 12B).

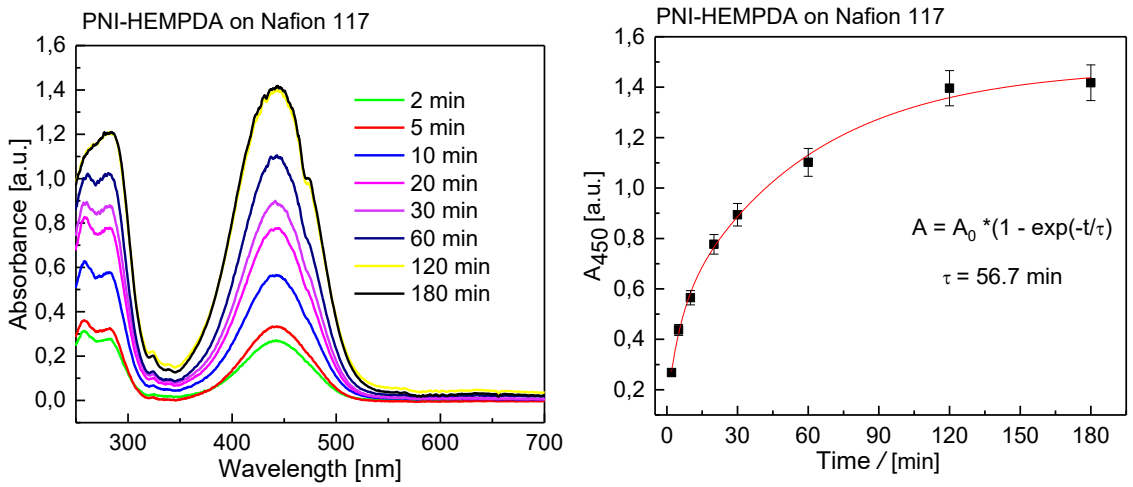

A B

Fig. 12: Absorption spectra of Nafion foil immersed in the solution of PNI-HEMPDA ($1.0 \cdot 10^{-4}$ M, 3.0 ml) (A) and values of absorbance at 450 nm plotted against time of binding (B)

The attachment of both CD and PNI-HEMPDA is schematically illustrated in Scheme 4:

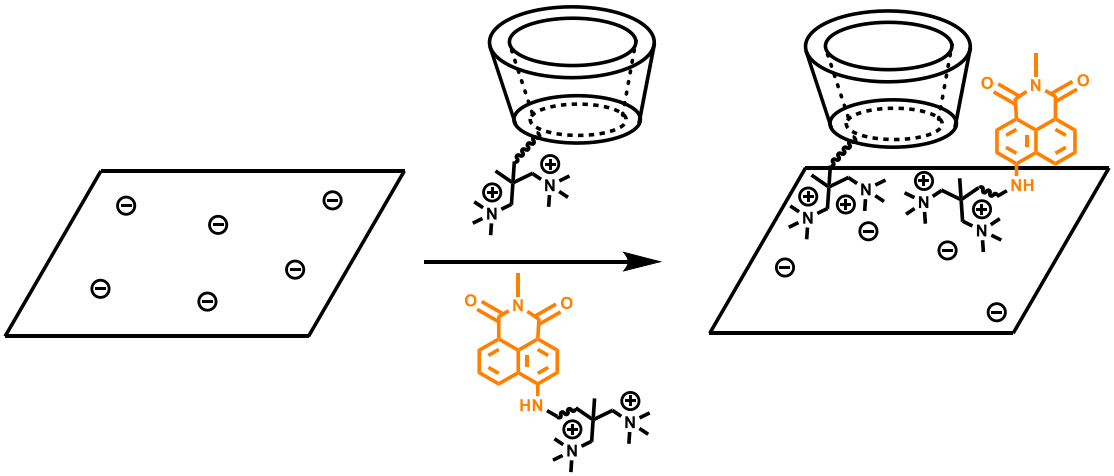

Scheme 4: Binding of PNI-HEMPDA and β-CD-TEEG-HEMPDA to Nafion

Nafion with bounded PNI-HEMPDA and β-CD-TEEG-HEMPDA was prepared (Scheme 4). Nafion was immersed in an equimolar solution of PNI-HEMPDA ($8.6 \cdot 10^{-4}$ M, 1.5 ml) and β-CD-TEEG-HEMPDA ($1.0 \cdot 10^{-4}$ M, 1.5 ml) for 120 minutes.

3.2.4 Attachment of fluorophores on Nafion 212

PNI-HEMPDA/Nafion® 212 composites were prepared by immersion of Nafion foil (10 x 10 mm) in a solution ($9.26 \cdot 10^{-5}$ M, 3.0 ml) of PNI-HEMPDA. The extent of fluorophore attachment was controlled by measurements of absorption spectra of the Nafion sheets as a function of immersion time (Fig. 13A). Values A_{450} of absorbance at 450 nm were plotted against the time of immersion and fitted with equation (3.2.3).
The time constant τ for the binding of PNI-HEMPDA to Nafion was 45.6 min (Fig. 12B).

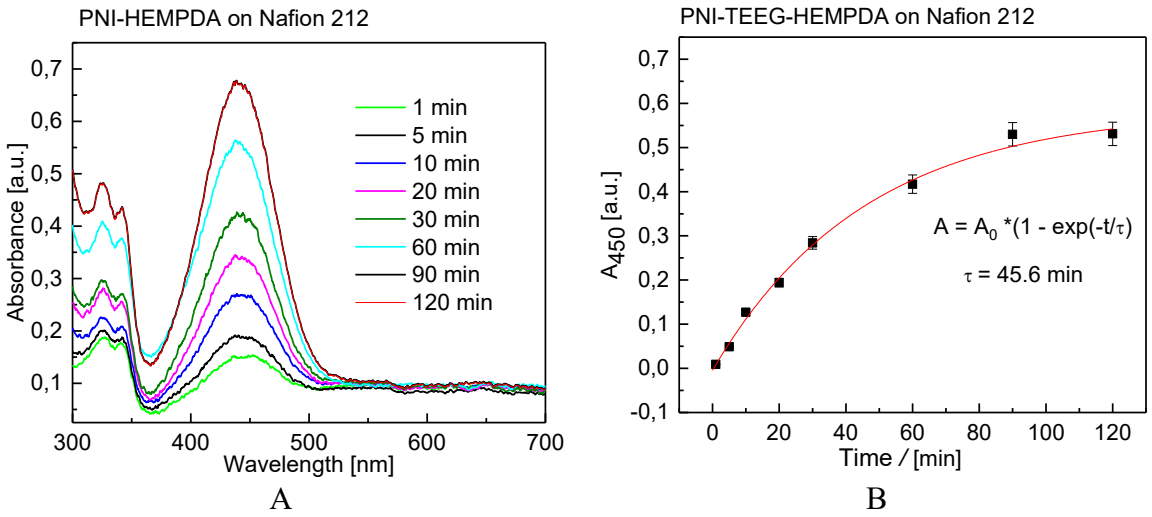

Fig. 13: Absorption spectra of Nafion foil immersed in the solution of PNI-HEMPDA ($1..0 \cdot 10^{-4}$ M, 3.0 ml) (A) and values of absorbance at 450 nm plotted against time of binding (B)

Subsequently, Nafion with bounded PNI-HEMPDA and β-CD-TEEG-HEMPDA was prepared. Nafion was immersed in an equimolar solution of PNI-HEMPDA ($9.26 \cdot 10^{-5}$ M, 1.5 ml) and β-CD-TEEG-HEMPDA ($9.30 \cdot 10^{-5}$ M, 1.5 ml) for 120 minutes.

3.3 Experimental setups

3.3.1 Measurement of UV/Vis absorption and fluorescence

UV/Vis absorption and fluorescence were measured using an optical fiber spectrometer AvaSpec ULS3648SEC (Avantes) equipped with a deuterium/halogen lamp AvaLight DHc and connected to an optical cuvette holder CUV-ALL/UV/VIS. Fluorescence was excited by a Flexpoint laser diode (5 mW, 405 nm), collected at 90° and detected after passing band-edge filter 430 nm.

3.3.2 Measurement of fluorescence sensor responses in the gas phase

Fluorescence sensor responses to various analytes in the gas phase were measured on a fluorescence setup combined with a system for preparation of precise concentration of studied analytes (Fig. 14). Fluorescence was excited by the 405 nm Flexpoint laser diode combined with a neutral filter (OD = 2.45) for attenuation of the laser light intensity. Light power on the sample was 15 μW, power density ~2 mW cm^{-2}. Fluorescence was collected at the angle of 90° to an optical fiber with a collimating lens, analyzed by a 20 cm HT20 monochromator (Jobin Yvon) and detected with a Hamamatsu R9836 photomultiplier. The signal from photomultiplier was amplified in a current preamplifier (Standford SR570), analyzed using a lock-in amplifier (Stanford SR830). Signal was processed using a National Instruments DAQ card using a program in the LabVIEW software environment.

The precise concentration of analytes for the measurements of fluorescence variations of our sensors in the presence of chemical species were prepared using an injection of a defined amount of analyte in a closed system with carrier gas circulation. A defined volume of analyte was injected with Hamilton syringe through the septum into a flask, which was thermostated at 100° C. A membrane pump was used for carrying the analyte vapors throughout the system. When the analyte met fluorescent glass beads in a 1/16” capillary or with functionalized Nafion in a holder, fluorescence intensity from the sensor element was changed and detected.

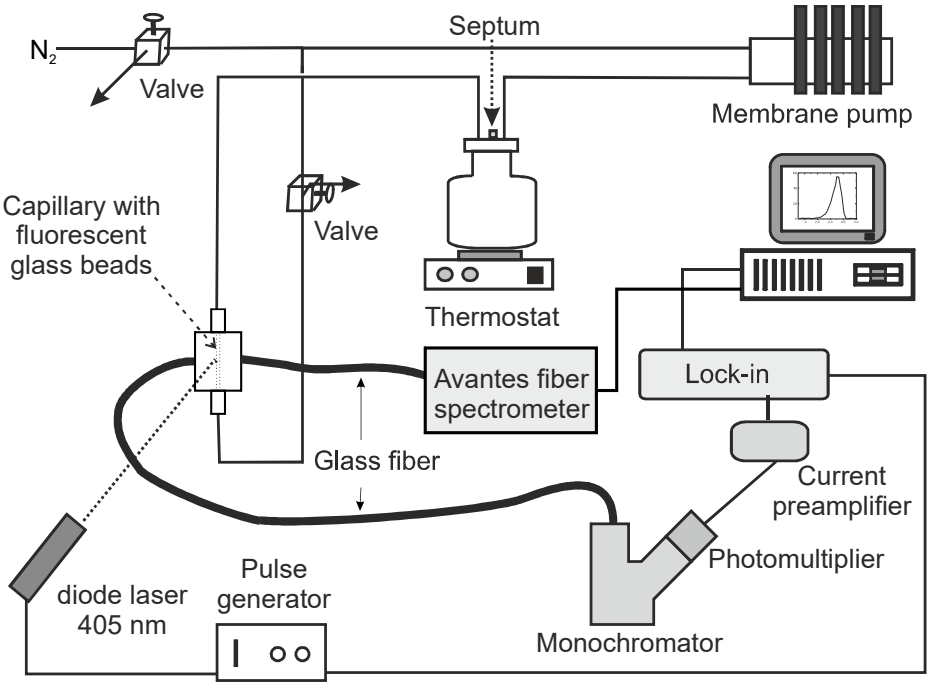

Fig. 14: Experimental setup for measurements of fluorescence sensor response in the gas phase

Fluorescence sensor responses to analytes in the gas phase were measured according to two methods.

3.3.2.1 Single concentration method

The selected analyte was introduced to the system operating in a closed-cycle mode, and the fluorescence intensity for a given analyte concentration was measured until the equilibrium value of fluorescence intensity was established. Afterward, the analyte was removed from the system by purging the system with nitrogen. This method enables to study fluorescence sensor response to a chosen analyte concentration together with the sensor response kinetics for this analyte concentration. For higher analyte concentrations the measurement time for a single concentration sensor response can be very long due to slow desorption of analyte from the sensor elements. In these cases, the sequential concentration method is a better choice.

3.3.2.2 Sequential concentration method

In this way of the preparation of analyte concentrations for fluorescence sensor response measurement, the analyte concentration is varied via subsequent additions of the liquid analyte into the system until the calibration dependence in a preferred concentration range is accomplished. During the measurement in this mode, a selected analyte was added to the sensor system operated in a closed-cycle mode, and the fluorescence intensity for a given analyte concentration was measured until the equilibrium value of fluorescence intensity was established. At this point, instead of purging the system with nitrogen, a new amount of the same analyte was added to the system, and the fluorescence sensor response was measured until equilibration of fluorescence intensity. The analyte additions were repeated until the saturation regime, or the desired concentration range was reached. The main advantage of this way is faster measurement without a need for purging the system with nitrogen after every addition of analyte. On the other hand, the actual concentration of the analyte is known less precisely as the errors of subsequent additions are added. The sensor response kinetics for a given total concentration realized in one step and several single steps may differ as well.

3.3.3 Measurement of fluorescence sensor responses in the liquid phase

Fluorescence sensor responses in the liquid phase were measured for systems with glass beads used as solid support. The experimental setup is schematically illustrated in Fig. 15.

For PNI-HEMPDA/GB based sensors - fluorophore functionalized glass beads in a 1/16" capillary - the fluorescence changes in the presence of liquid analytes were measured using an experimental setup in Fig. 15. Liquid analytes were transported to the capillary using an HPLC pump (LCP5020, Ingos). Fluorescence was continuously detected at fluorescence maximum (540 nm) during the flow of analytes and water through the capillary with fluorescent glass beads.

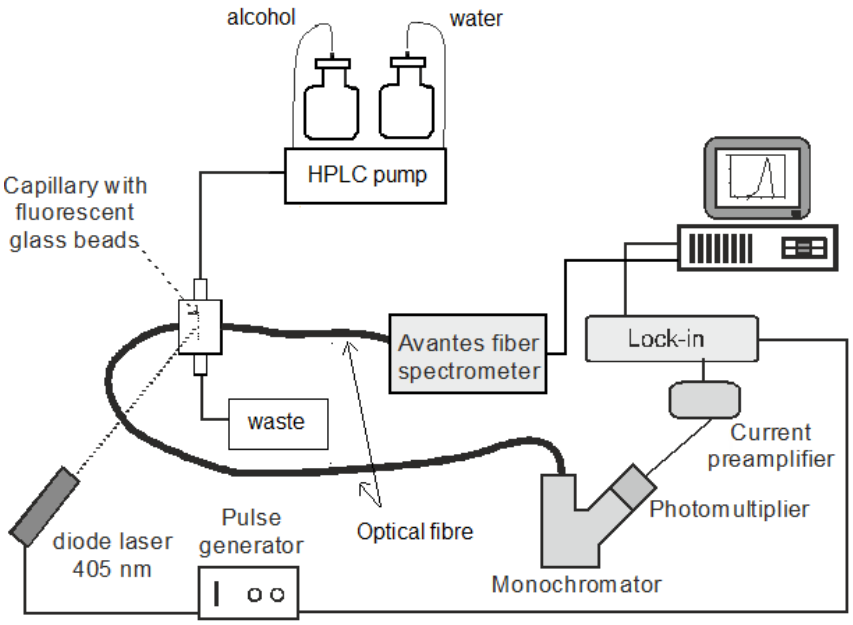

Fig. 15: Experimental setup for measurements of fluorescence sensor response for PNI-HEMPDA/GB in the liquid phase.

4 RESULTS AND DISCUSSION

4.1 Naphthalimide derivative on glass beads

4.1.1 Fluorescence responses of PNI-HEMPDA/GB sensors in the liquid phase

Fluorescence sensor response of PNI-HEMPDA/GB to analytes in the liquid phase was measured for a homological set of linear alcohols from methanol to 1-pentanol. Fluorescence was continuously detected as a function of time during the flow of analytes and water. Fluorescence intensities at 540 nm in the presence of the studied analytes were higher than the fluorescence intensity in water. The time evolution of sensor response was repeated four times for each analyte (Fig. 16).

Time dependencies of fluorescence intensity I_{450} at 540 nm were fitted with exponential growth function for monomolecular kinetics:

$$I_{540} = I_0 + I_{max} \cdot \left(1 - e^{-\frac{(t-t_0)}{\tau}}\right) \quad (4.1.1)$$

where I_0 is the fluorescence signal corresponding to the baseline of water, t_0 is time when analyte arrived at the measuring spot in the sensing capillary, I_{max} is the maximum of fluorescence change due to the presence of analyte and τ is the time constant of the fluorescence sensor response (in the approximation of a first-order kinetics).

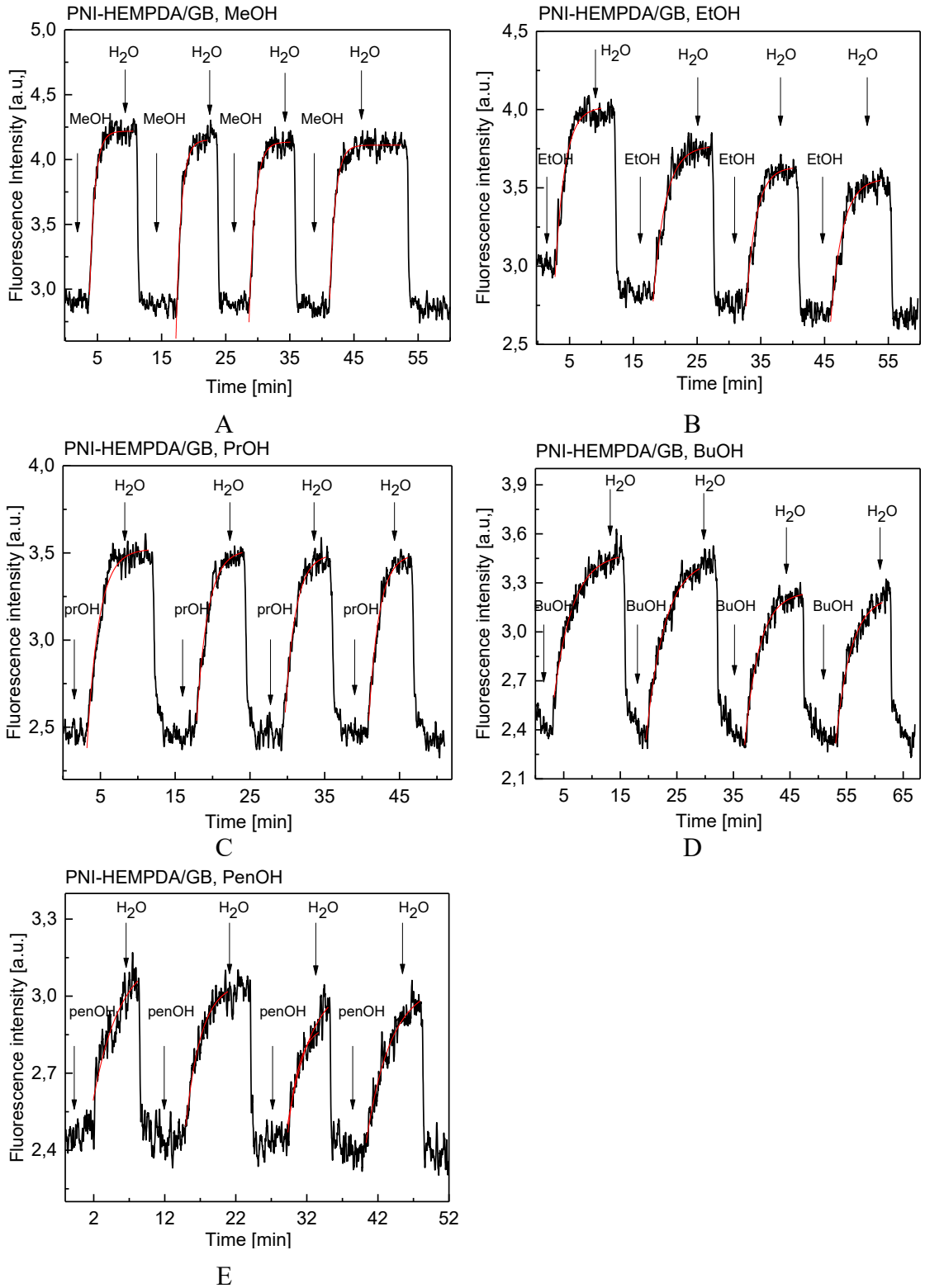

Fig. 16: Liquid-phase fluorescence sensor responses of PNIAHA/GB to methanol (A), ethanol (B), propanol (C), 1-butanol (D) and 1-pentanol (E) and evaluation of time constants for alcohols (F), fitted with the use of equation 4.1.

Calculated sensor response time constants for each analyte and measurement are in Tab. 3.

The graph Fig. 17A shows repeatability of evaluated sensor response time constants and their comparison for alcohols. Results for methanol, ethanol, propanol, and 1-butanol show reasonable repeatability for each measurement, only results for 1-pentanol were different, probably due to the slight instability of the solid phase.

Values sensor response time constants are plotted against a number of carbons in the chain of alcohols in the graph Fig. 17B. It illustrates that in the homologous series of linear alcohols, sensor response time constants increase with the number of carbons in the chain. The reason for this increase is that bigger molecules of analytes need more extended time for the interaction with a fluorophore. Another reason can be the polarity effect; more polar alcohols interact better with the polar surface of Nafion.

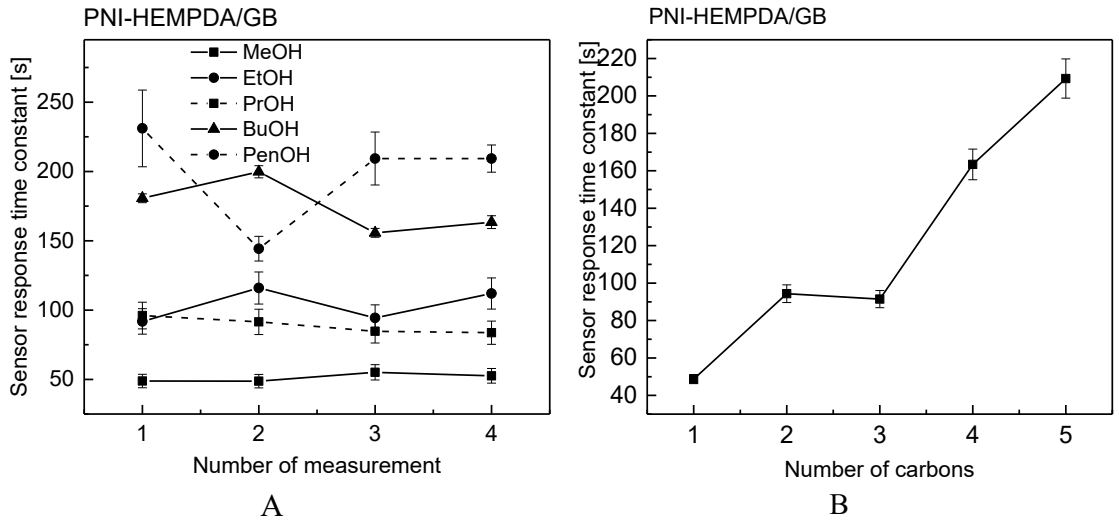

Fig. 17: Values of sensor response time constants plotted against a number of measurement and number of carbons for linear alcohols.

Tab. 3: Values of sensor response time constants for every analyte and measurement for PNIAHA/GB in the liquid phase.

	sensor response time constants / s				
analyte	1.	2.	3.	4.	$\tilde{x}$
methanol	48.8±0.9	48.7±1.0	55.1±1.0	52.6±0.9	48.8
ethanol	91.8±2.3	116±3.1	94.3±2.8	112±2.5	98,4
propanol	96.0±2.1	91.4±2.3	84.7±2.5	83.7±2.4	84.7
1-butanol	181±3.2	200 ±4.4	156±3.2	163±4.6	163
1-pentanol	231±7.6	144±8.9	209±19	209±3.8	209

Furthermore, values of fluorescence intensity in alcohols and water were plotted into column graphs (Fig. 19) for better illustration of the repeatability of measurements. Relative fluorescence sensor response *R* was evaluated according to the equation 4.1.2:

$$R = \frac{I_{H_2O} - I_{ROH.}}{I_{H_2O}}, \qquad (4.1.2)$$

where I_{H_2O} is fluorescence intensity of PNI-HEMPDA/GB in water, I_{ROH} is fluorescence intensity of PNI-HEMPDA/GB in a particular alcohol. Results are plotted for each measurement in Fig. 18 and show good repeatability for linear alcohols except for 1-butanol. According to the results of pair *t*-test, values of relative fluorescence quenching are significantly different at α = 0.05 for each alcohol.

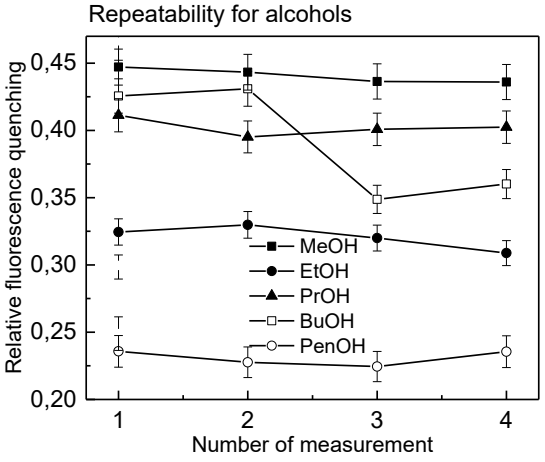

Fig. 18: Repeatability of fluorescence sensor response of PNI-HEMPDA/GB to linear alcohols.

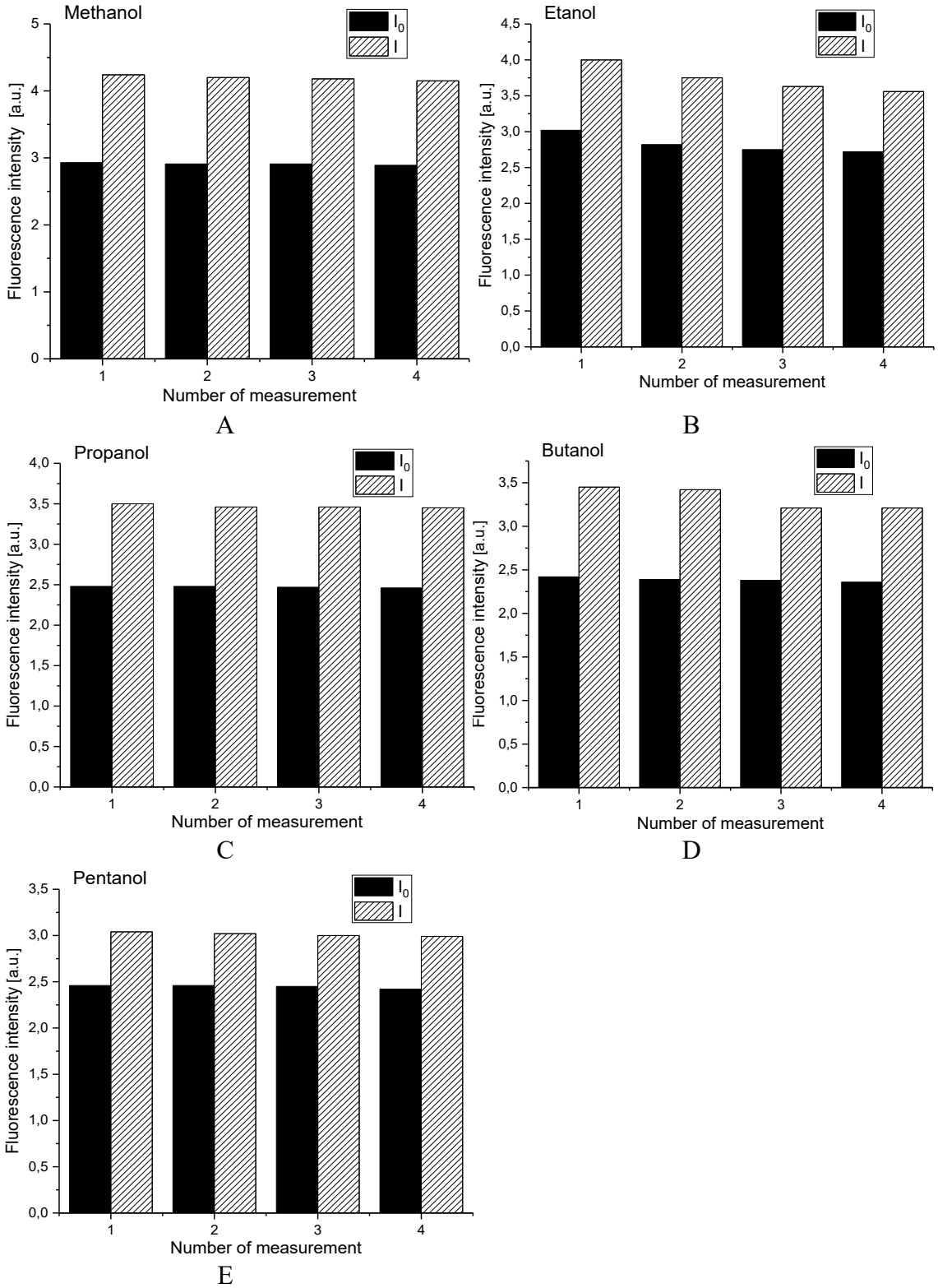

Fig. 19: Repeatability of fluorescence responses of PNI-HEMPDA/GB sensor to methanol (A), ethanol (B), 1-propanol (C), 1-1-butanol (D) and 1-1-pentanol (E) and comparison of relative fluorescence quenching for linear alcohols (F).

4.1.2 Fluorescence responses of PNI-HEMPDA/GB sensors in the gas phase

Fluorescence sensor responses to ethanol were measured according to sequential concentration method. Resulting dependencies of fluorescence intensity on time for Nafion with PNI-HEMPDA, β-CD-HEMPDA and γ-CD -HEMPDA are in Fig. 20. Volumes and times of addition for every analyte are marked in graphs with arrows.

Relative fluorescence quenching response R to ethanol was evaluated according to the equation 4.1.3:

$$R = \frac{I_0 - I}{I_0}, \qquad (4.1.3)$$

where I_0 is initial fluorescence intensity before the addition of an analyte, I is fluorescence intensity after addition of an analyte and relative fluorescence quenching express change in fluorescence intensity caused by the analyte.

Dependences of relative fluorescence quenching on the concentration of ethanol for glass beads with PNI-HEMPDA, β-CD + PNI-HEMPDA and γ-CD + PNI-HEMPDA are plotted in Fig. 20D. Values for glass beads with only PNI-HEMPDA and PNI-HEMPDA with β-CD or γ-CD + PNI-HEMPDA are slightly different, but no changes in sensor response due to interaction with CD can be observed.

As can be seen in Fig. 20 A-C, fluorescence intensity is decreasing in time because of photobleaching of PNI-HEMPDA on the surface of glass beads.

For these reasons, we had chosen a Nafion membrane for further experiments instead of glass beads. We expected that a considerably higher amount of PNI-HEMPDA could be attached to the surface of Nafion, so interactions with CD could be observable and photobleaching should be less problematic.

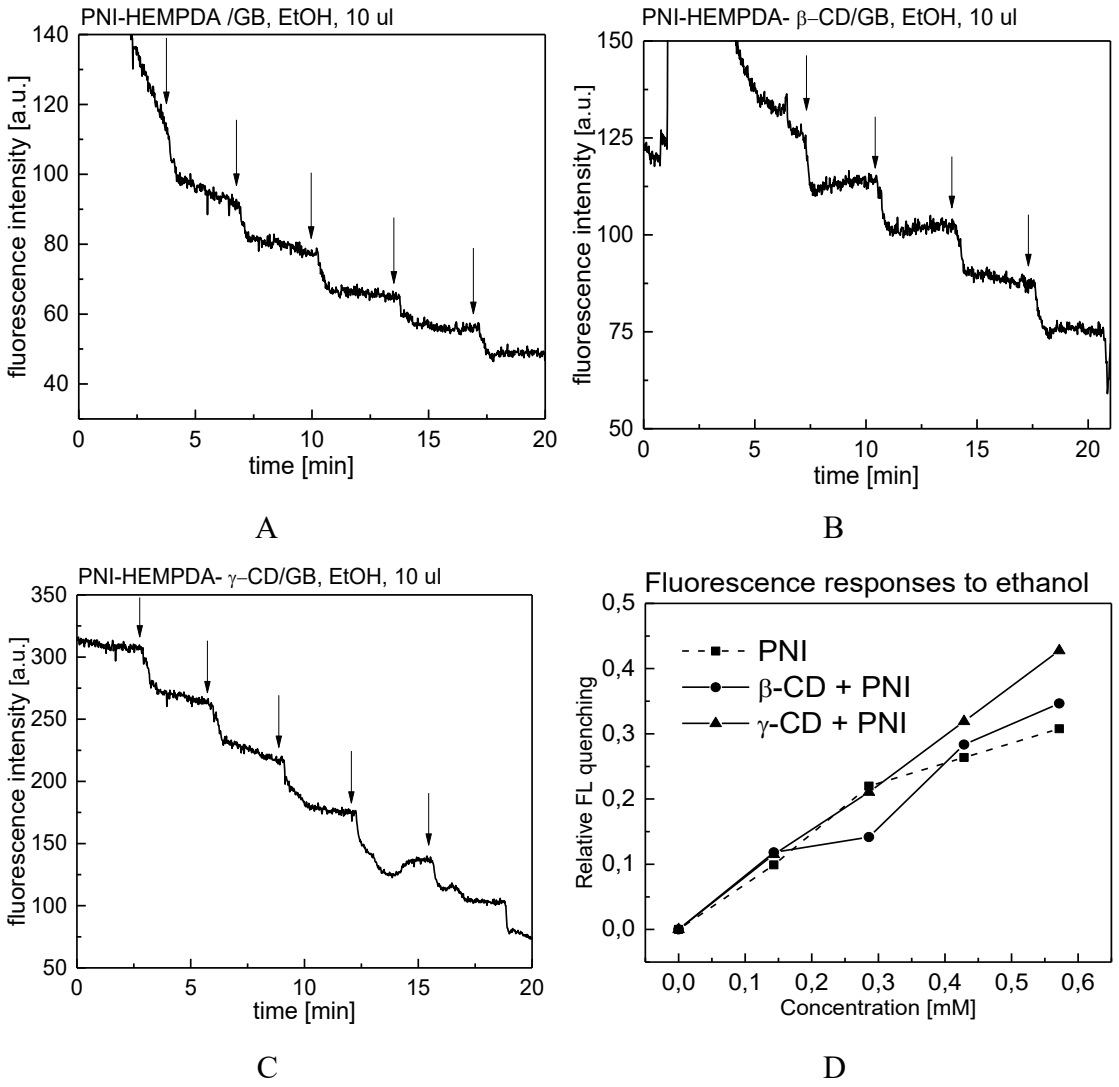

Fig. 20: Fluorescence sensor responses to ethanol for PNI-HEMPDA (A), PNI-HEMPDA and β-CD (B), PNI-HEMPDA and γ-CD (C) and evaluation of relative fluorescence quenching (D)

4.2 Naphthalimide derivatives/Nafion® 117

4.2.1 Fluorescence sensor response of the PNI/Nafion 117 in the gas phase

Fluorescence sensor responses were measured for methanol, ethanol, and 1-pentanol vapors. Results for PNI-HEMPDA /Nafion 117 are in Fig. 21 and for Nafion with both PNI-HEMPDA and β-CD-TEEG-HEMPDA in Fig. 22. Injections of corresponding analyte volumes to the measurement system are indicated with arrows.

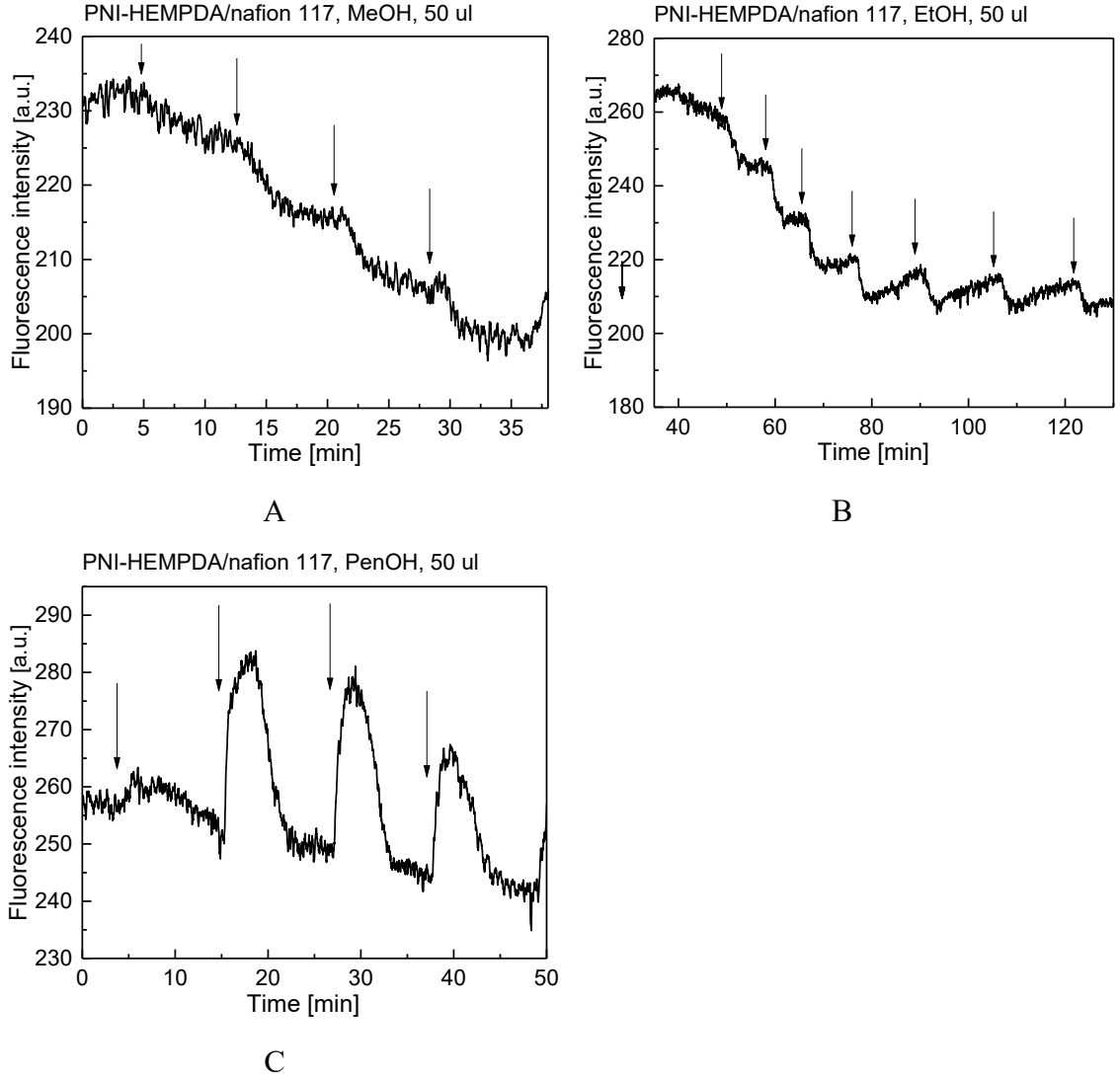

Fig. 21: Gas-phase fluorescence sensor responses for PNI-HEMPDA to selected alcohols: methanol (A), ethanol (B), 1-pentanol (C).

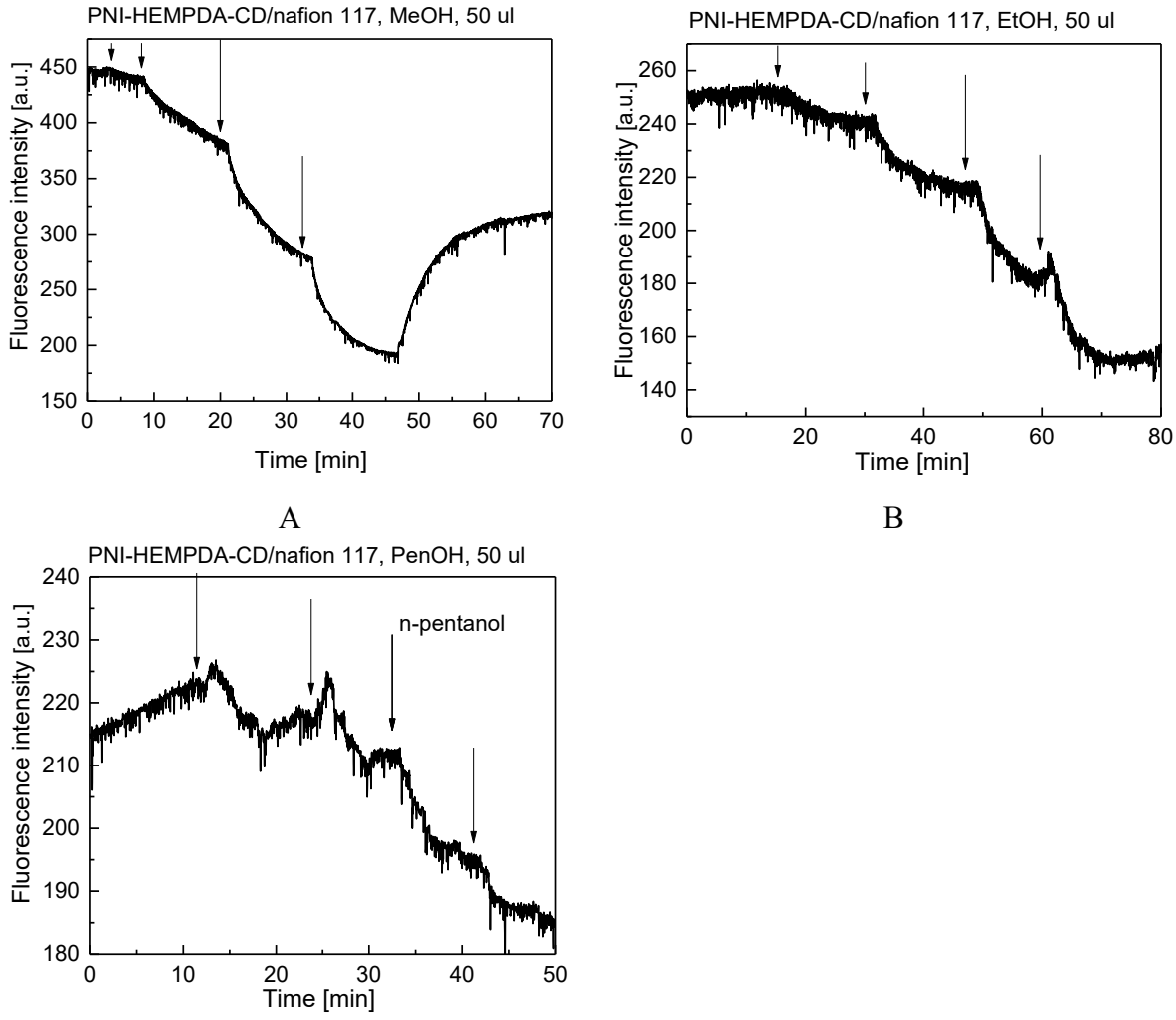

Fig. 22: Gas-phase fluorescence sensor responses for PNI-HEMPDA with β-CD-HEMPDA to selected alcohols: methanol (A), ethanol (B), 1-pentanol (C).

Relative fluorescence quenching of PNI-HEMPDA/Nafion 117 sensor elements to selected alcohols was evaluated for both samples according to the equation 4.1.3.

Values of relative fluorescence quenching were plotted against the concentration of analytes and resulting dependencies for samples Nafion 117/PNI-HEMPDA and Nafion 117/PNI-HEMPDA+β-CD are in (Fig. 23).

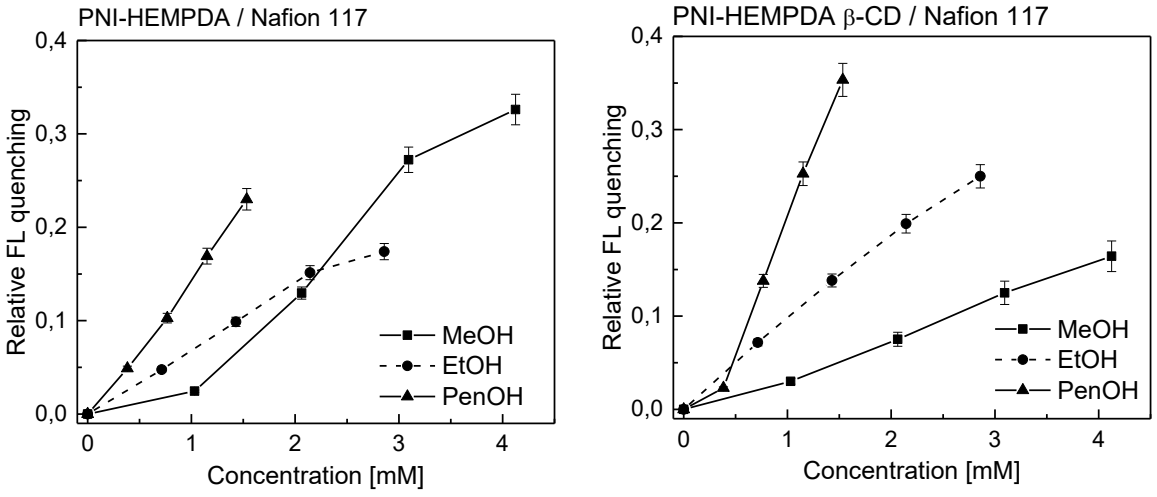

A B

Fig. 23: Evaluation of relative fluorescence quenching for Nafion 117 with PNI-HEMPDA (A), both PNI-HEMPDA and β-CD-HEMPDA (B) and comparison for both samples (C)

As can be seen in Fig. 23B, the presence of β-CD caused a significant change in relative fluorescence quenching, and linear alcohols were better differentiated.

Subsequently, changes in fluorescence intensity were plotted against change in concentration. The sensitivity *S* of the sensor response was then calculated as the slope of the dependence:

$$S = \frac{\Delta R}{\Delta c} \tag{4.2.1}$$

where ΔR is a change in fluorescence intensity before and after addition of an analyte, Δc is a change of concentration of the detected analyte. Values of the sensitivity of PNI-HEMPDA and PNI-HEMPDA + β-CD sensor response to linear alcohols are in (Tab 4).

Tab. 4: Sensitivity of Nafion 117/PNI-HEMPDA and PNI-HEMPDA + β-CD sensor responses to linear alcohols.

analyte	$\boldsymbol{S}$ / $\mathrm{mmol^{-1} \cdot dm^3}$	
	PNI-HEMPDA	**PNI-HEMPDA + β-CD**
methanol	0.087 ± 0.011	0.041 ± 0.002
ethanol	0.063 ± 0.004	0,076 ± 0.004
1-pentanol	0.151 ± 0.005	0,244 ± 0.026

Consequently, the limit of detection (c_{LOD}) was calculated from the equation:

$$c_{LOD} = \frac{2\frac{\Delta I_n}{I_0}}{S}, \tag{4.2.2}$$

where ΔI_n is a maximum baseline fluctuation, I_0 is the value of fluorescence intensity before the first addition of an analyte, and *S* is the sensitivity calculated from the equation (4.2.1).

Tab. 5: LOD for Nafion 117/PNI-HEMPDA and PNI-HEMPDA + β-CD sensor responses to linear alcohols.

analyte	c_{LOD} / mmol · dm^{-3}	
	PNI-HEMPDA	**PNI-HEMPDA + β-CD**
methanol	0.610	0.929
ethanol	0.861	0.493
1-pentanol	0.427	0.162

As follows from results in Tab. 4, the sensitivity of Nafion 117/PNI-HEMPDA + β-CD to ethanol and 1-pentanol is higher than the sensitivity of Nafion 117/PNI-HEMPDA and dependencies of relative fluorescence quenching are better differentiated. These changes indicate that β-CD is acting as a recognized part of the sensor.

However, as photobleaching is still significant and values of noise are high, Nafion 212 membrane was used for further experiments instead of Nafion 117. Given that Nafion 212 is considerably thicker, analytes can get into contact with sensor faster and more sensitive responses could be achieved.

4.3 Nafion® 212

4.3.1 Fluorescence sensor response of PNI/Nafion 212 in the gas phase

Firstly, fluorescence sensor responses were measured for a wide variety of organic analytes, to examine PNI-HEMPDA sensor potential scope of application.

For nonpolar analytes – benzene, toluene, hexane, dichloromethane, chloroform – no sensor responses were detected, which was probably caused by their reluctance to interact with the polar surface of Nafion.

Aprotic polar analytes – acetonitrile, acetone, ethyl acetate, tetrahydrofuran – did not cause any change in fluorescence intensity of PNI-HEMPDA as well.

However, protic polar compounds caused considerable changes in fluorescence intensity, and the use of PNI-HEMPDA/Nafion system for their detection seems to be promising.

Fluorescence sensor responses to the homological series of alcohols from methanol to 1-hexanol were measured with both sequential and single concentration method.

4.3.1.1 PNI/Nafion 212 measured with sequential concentration method

For sequential concentration method, resulting dependances of fluorescence intensity on time for Nafion with PNI-HEMPDA are in Fig. 24 and for Nafion with both PNI-HEMPDA and β-CD -HEMPDA in Fig. 25.

Volumes and times of addition for every analyte are marked in graphs with arrows.

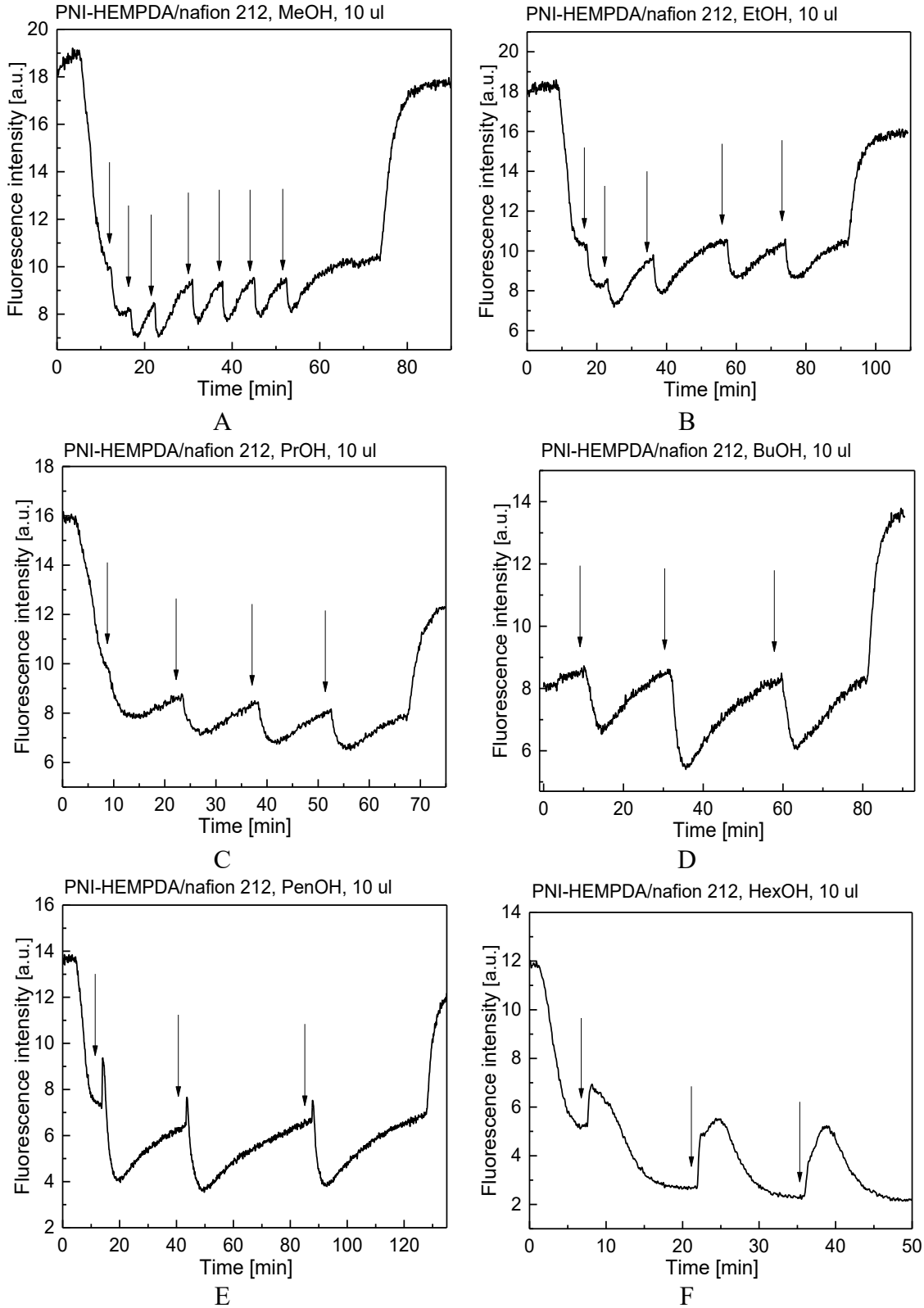

Fig. 24: Fluorescence sensor responses for PNI-HEMPDA to selected alcohols: methanol (A), ethanol (B), propanol (C), 1-butanol (D), 1-pentanol (E) and 1-hexanol (F).

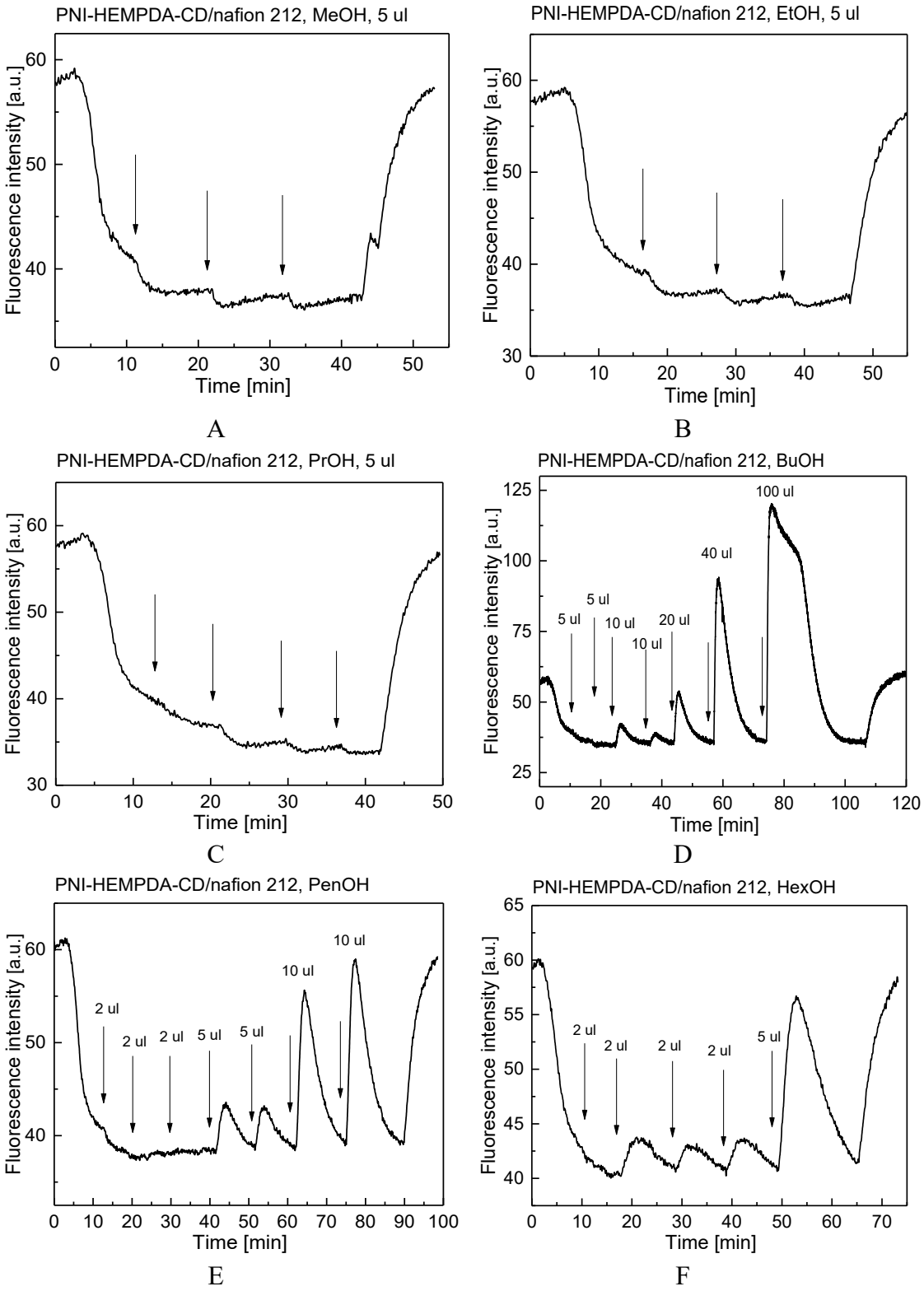

Fig. 25: Fluorescence sensor responses for PNI-HEMPDA with β-CD to selected alcohols: methanol (A), ethanol (B), propanol (C), 1-butanol (D), 1-pentanol (E) and 1-hexanol (F).

Relative fluorescence quenching of PNI-HEMPDA to linear alcohols was then evaluated according to the equation 4.1.3.

Values of relative fluorescence quenching were plotted against the concentration of analytes and resulting dependencies for samples Nafion 212/PNI-HEMPDA and Nafion 212/PNI-HEMPDA+β-CD are in Fig. 26.

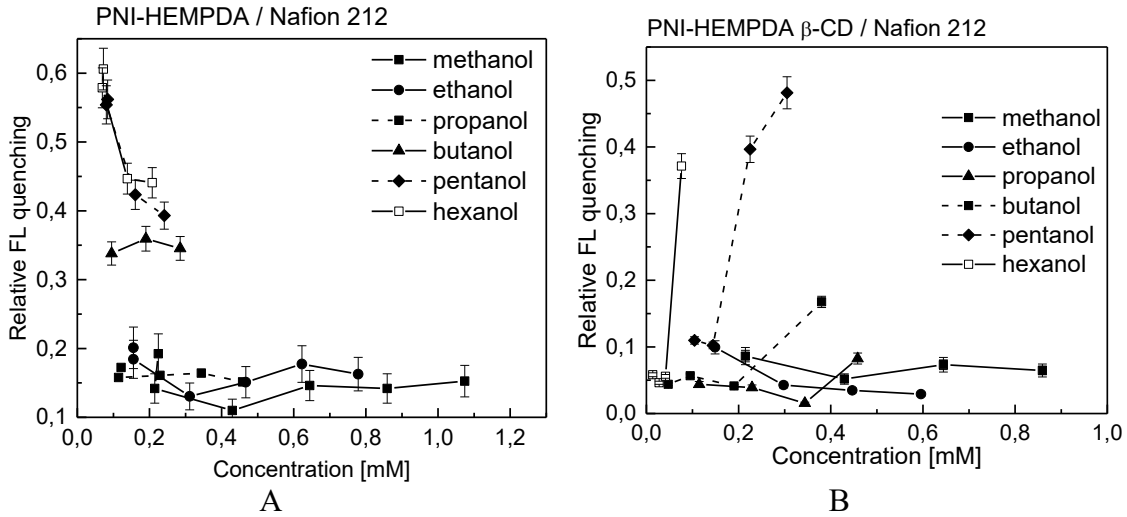

Fig. 26: Evaluation of relative fluorescence quenching for Nafion 212 with PNI-HEMPDA (A), and both PNI-HEMPDA and β-CD-HEMPDA (B) measured with sequential concentration method.

However, as can be seen in Fig. 26, dependences of relative fluorescence quenching to concentration are not linear even for the low concentrations and sensor´s parameters cannot be calculated precisely. For this reason, measurements were repeated with a single concentration method.

4.3.1.2 PNI/Nafion 212 measured with single concentration method

The single concentration method was used for these experiments when analyte was removed from the system by purging with nitrogen after every addition. Therefore, the concentration of the analyte in time corresponded to the actual volume of analyte which was introduced to the system.

Resulting dependencies of fluorescence intensity on time for Nafion with PNI-HEMPDA are in Fig. 27 and for Nafion with both PNI-HEMPDA and β-CD-TEEG-HEMPDA are in Fig. 28.
Volumes and times of addition for every analyte are marked in graphs with arrows up, arrows down indicate times when the system was purged with nitrogen.

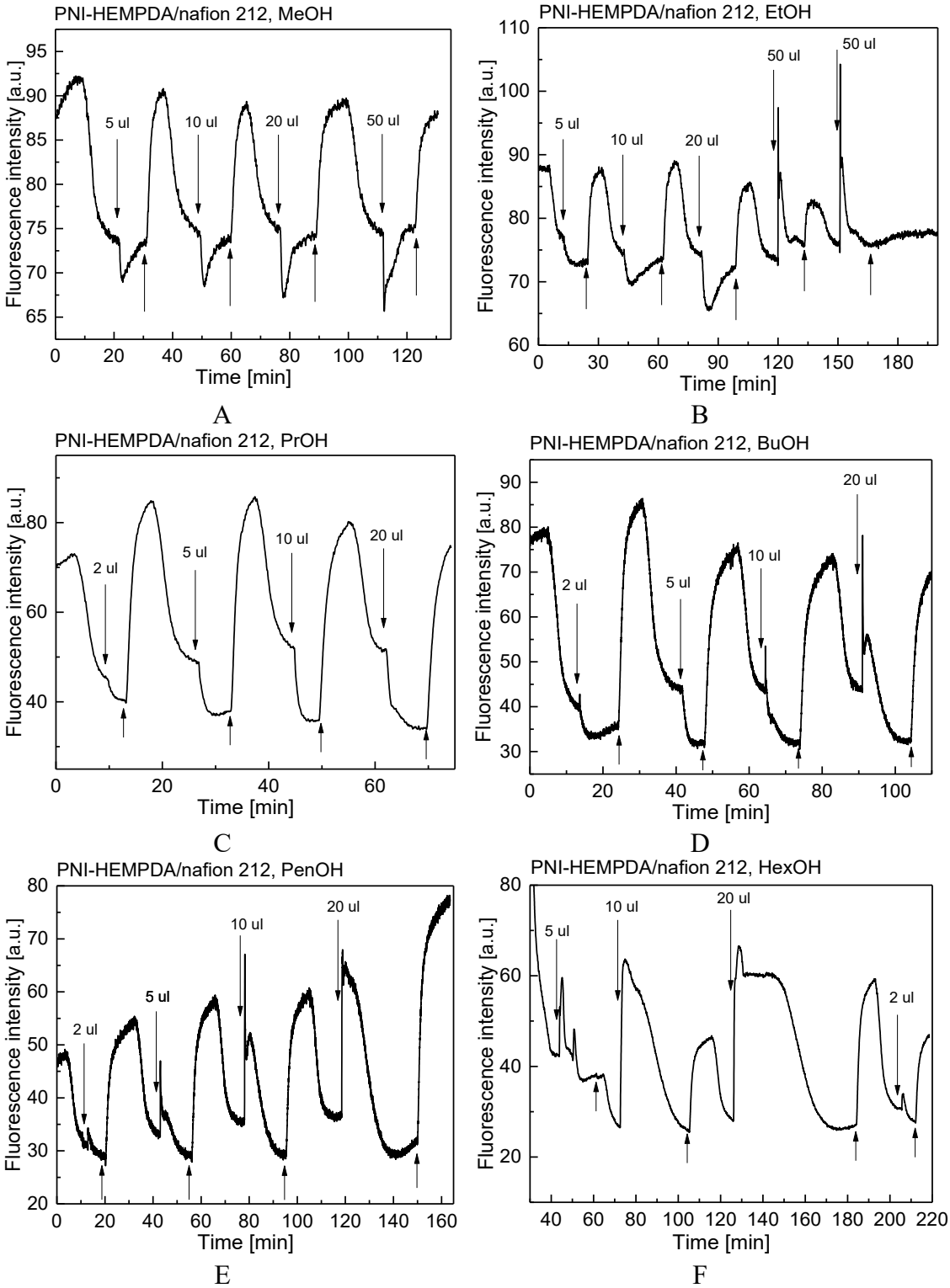

Fig. 27: Fluorescence sensor responses for PNI-HEMPDA to selected alcohols: methanol (A), ethanol (B), propanol (C), 1-butanol (D), 1-pentanol (E) and 1-hexanol (F).

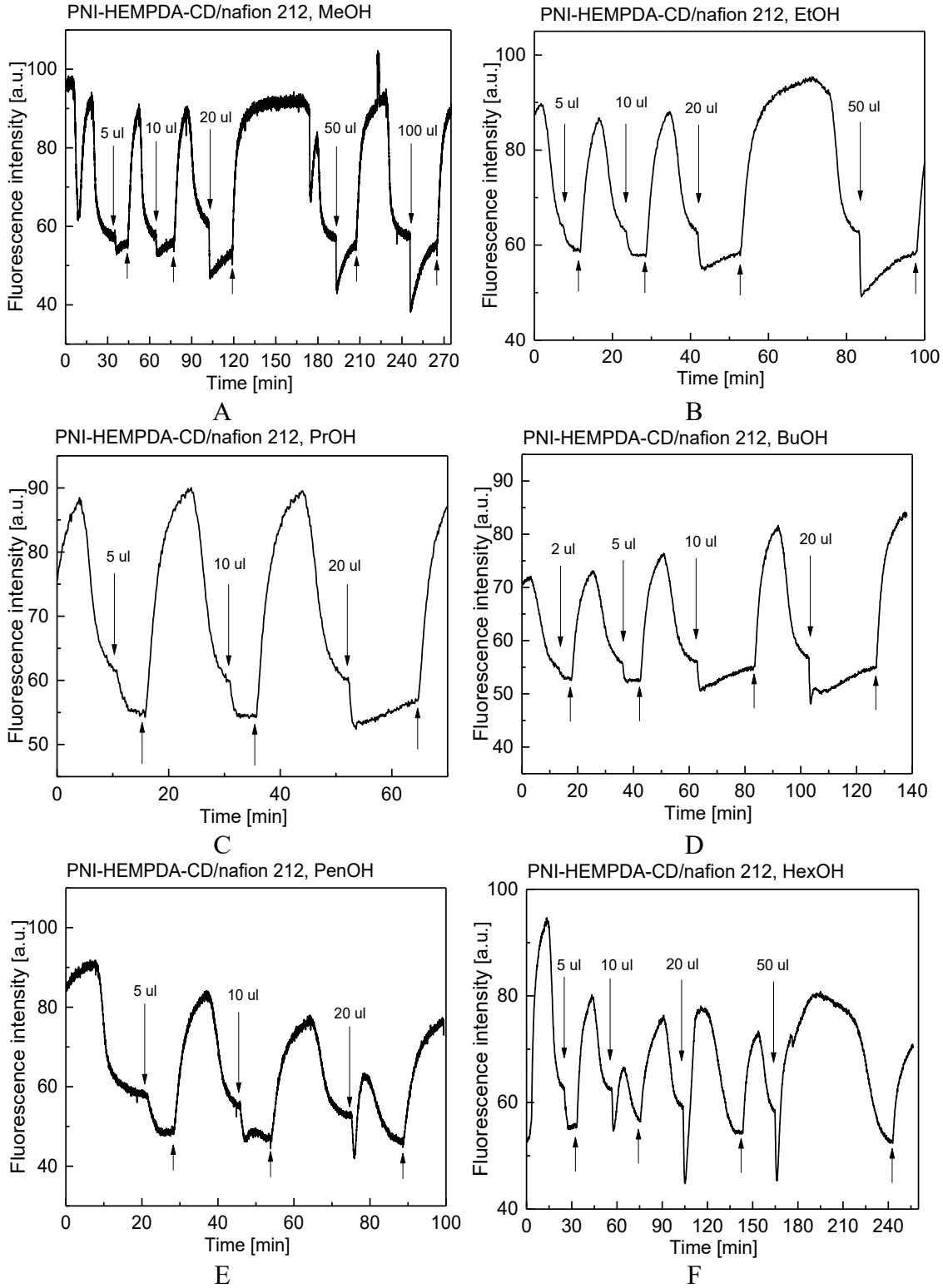

Fig. 28: Fluorescence sensor responses for PNI-HEMPDA and β-HEMPDA to selected alcohols: methanol (A), ethanol (B), propanol (C), 1-butanol (D), 1-pentanol (E) and 1-hexanol (F).

Relative fluorescence quenching of PNI-HEMPDA to linear alcohols was then evaluated according to the equation 4.1.3.

Values of relative fluorescence quenching were plotted against the concentration of analytes and resulting dependencies for samples Nafion 212/PNI-HEMPDA and Nafion 212/PNI-HEMPDA+β-CD are in Fig. 29.

As follows from dependencies (Fig. 29), values of relative fluorescence quenching are increasing with decreasing polarity of linear alcohols. However, the linear dynamic range of PNI-HEMPDA and PNI-HEMPDA + β-CD sensor responses to linear alcohols (Tab. 8) decrease with decreasing polarity of linear alcohols.

The reason for these trends is presumably that surface of Nafion 212-based sensors get saturated with increasing concentration of less polar alcohols, and therefore the sensor response is no longer linear.

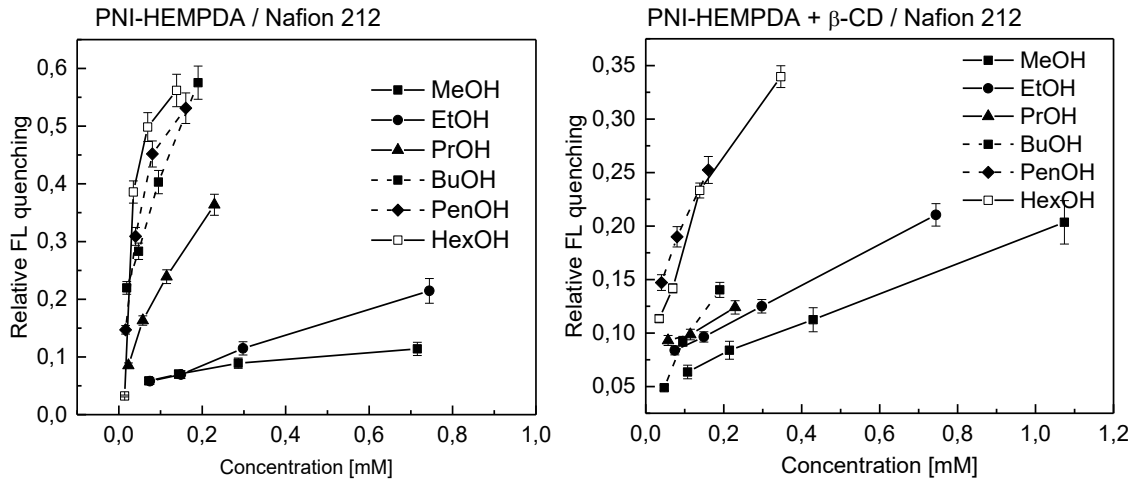

Fig. 29: Evaluation of relative fluorescence quenching for Nafion 212 with PNI-HEMPDA (A), and both PNI-HEMPDA and β-CD-HEMPDA (B) measured with a single concentration method.

Subsequently, changes in fluorescence intensity were plotted against change in concentration. The sensitivity of the sensor was then calculated as the from equation 4.2.1. Values of the sensitivity of PNI-HEMPDA and PNI-HEMPDA + β-CD sensor responses to linear alcohols are in Tab. 6.

Tab. 6: Sensitivity of PNI-HEMPDA and PNI-HEMPDA + β-CD sensor responses to linear alcohols.

analyte	S / $\mathrm{mmol^{-1} \cdot dm^3}$	
	PNI-HEMPDA	**PNI-HEMPDA + β-CD**
methanol	0.08 ± 0.01	0.14 ± 0.003
ethanol	0.24 ± 0.01	0.19 ± 0.002
propanol	1.30 ± 0.13	0.19 ± 0.03
1-butanol	1.81 ± 0.10	0.62 ± 0.10
1-pentanol	2.42 ± 0.56	0.86 ± 0.07
1-hexanol	2.04 ± 1.06	1.17 ± 0.12

LOD was then calculated from the equation (4.2.2), and results are in Tab. 7.

Tab. 7: LOD for Nafion 117/PNI-HEMPDA and PNI-HEMPDA + β-CD sensor responses to linear alcohols.

analyte	$\boldsymbol{LOD}$ / $\cdot 10^{-1}\mathrm{mmol\ dm^{-3}}$	
	PNI-HEMPDA	PNI-HEMPDA + β-CD
methanol	0.317	0.480
ethanol	0.131	0.207
propanol	0.050	0.104
1-butanol	0.048	0.046
1-pentanol	0.043	0.078
1-hexanol	0.024	0.041

The linear dynamic range of PNI-HEMPDA and PNI-HEMPDA + β-CD sensor responses to linear alcohols was calculated according to the equation (4.2.2).

Tab. 8: Linear dynamic range of PNI-HEMPDA and PNI-HEMPDA + β-CD sensor responses to linear alcohols

analyte	*Linear dynamic range* / $\mathrm{mmol \cdot dm^{-3}}$	
	PNI-HEMPDA	**PNI-HEMPDA + β-CD**
methanol	0.07 – 0.72	0.07 – 1.10
ethanol	0.07 – 0.75	0.07 – 0.75
propanol	0.06 – 0.23	0.06 – 0.23
1-butanol	0.05 – 0.22	0.05 – 0.22
1-pentanol	0.08 – 0.16	0.04 – 0.16
1-hexanol	0.10 – 0.14	0.07 – 0.14

4.3.2 Application of PNI/Nafion 212 for a determination of ethanol in heptane

The determination of ethanol in gasoline with Nafion 212/ PNI-HEMPDA + β-CD sensor system was realized with mixtures of ethanol with heptane; heptane was used as a substitute for gasoline. The single concentration method described above was used for quantification of ethanol in heptane.

Resulting dependencies of fluorescence intensity on time for Nafion with PNI-HEMPDA and β-CD-TEEG-HEMPDA are in Fig. 30. Volumes and times of addition for every analyte are marked in graphs with arrows up, arrows down indicate times when the system was purged with nitrogen.

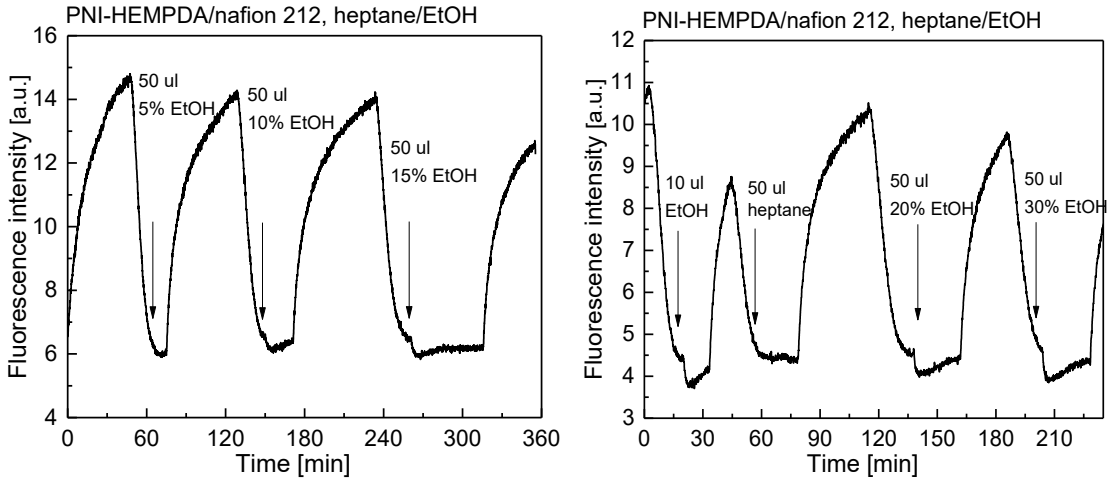

Fig. 30: Fluorescence sensor responses for PNI-HEMPDA + β-CD to ethanol in heptane at different volume concentrations.

Relative fluorescence quenching of PNI-HEMPDA to ethanol was then evaluated according to the equation 4.1.3.

Values of relative fluorescence quenching were plotted against the volume concentration of ethanol, and resulting dependences are in (Fig. 31).

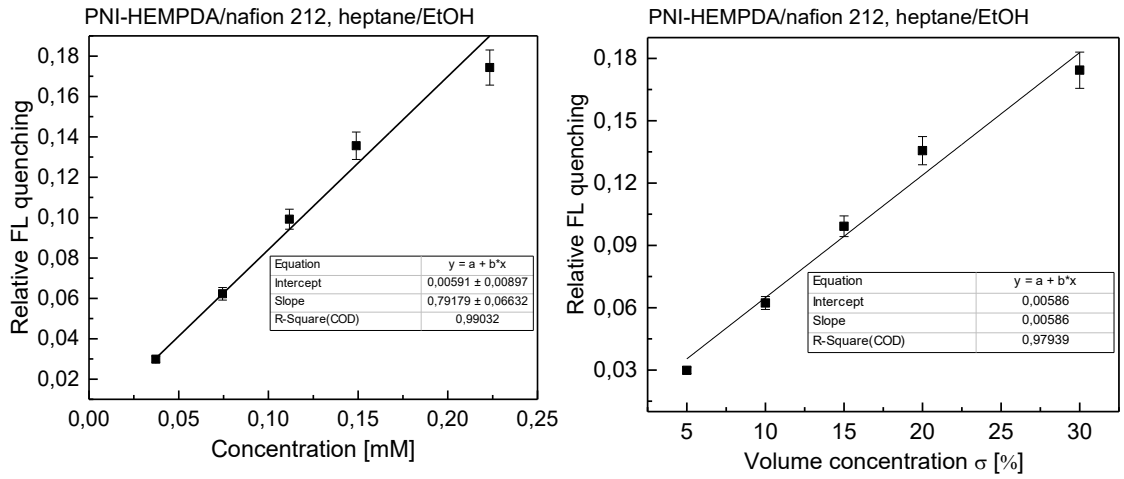

A B

Fig. 31: Dependence of relative fluorescence quenching on a molar (A) and volume (B) concentration of ethanol in heptane.

The calibration line obtained by linear fitting of (Fig. 31A) is the following:

$$R = 0.00591 - 0.7918 \cdot c_{EtOH}, \qquad (4.2.3)$$

where R is relative fluorescence quenching response to ethanol and c_{EtOH} is a volume concentration of ethanol in heptane.

The sensitivity of the sensor was then calculated from the slope of dependence (4.2.1), and *LOD* was calculated according to the equation (4.2.2). Sensitivity *S* was (0.791 ± 0.066) mmol$^{-1} \cdot$ dm^3 and *LOD* was 0.0574 mmol dm^{-3}. Linear dynamic range was confirmed in the whole calibration range 0.037 – 0.223 mmol dm^{-3}.

5 CONCLUSIONS

In this thesis, a new fluorescent sensor system based on naphthalimide and cyclodextrin derivatives attached to solid support was developed. The following tasks were successfully fulfilled:

1. Synthesis of positively charged naphthalimide derivatives PNI-HEMPDA.
2. Chemical modification of glass beads surfaces via the creation of negatively charged sulfonate groups; determination of the extent of surface modification using UV-VIS spectroscopy.
3. Preparation of the fluorosensor systems without or with charged cyclodextrin derivatives for gas and liquid phase:
   - glass beads/PNI-HEMPDA, glass beads/PNI-HEMPDA+CD
   - Nafion 117/PNI-HEMPDA, Nafion 117/PNI-HEMPDA+CD
   - Nafion 212/PNI-HEMPDA, Nafion 212/PNI-HEMPDA+CD
4. Measurements of fluorescence sensor responses of the prepared sensors in the gas and liquid phase to linear alcohols using sequential and/or single concentration method.
5. Static parameters – sensitivity, limit of detection, linear dynamic range – were determined from the concentration dependence of the fluorescence sensor response. A dynamic parameter – sensor response time constant – was determined for fluorescence response of glass beads/PNI-HEMPDA in the liquid phase.
6. The novel fluorosensor system for the detection of ethanol in gasoline was examined. Nafion 212/PNI-HEMPDA + β-CD sensor system was used for the determination of ethanol in model heptane. The linear dependence of relative fluorescence quenching to the concentration of ethanol makes this method promising for quick quantification of ethanol in gasoline.

6 REFERENCES

[1] T. Ogoshi; A. Harada: Chemical Sensors Based on Cyclodextrin Derivatives. *Sensors (Basel, Switzerland)* **8**:8, 4961-4982 (2008).

[2] J. Lakowicz; (ed.): *Principles of Fluorescence Spectroscopy*, 2006.

[3] P. Atkins; J. De Paula; (ed.): *Physical Chemistry: Thermodynamics, structure, and change 8th ed*, Oxford: Oxford University Press 2006.

[4] H. Sahoo: Förster resonance energy transfer – A spectroscopic nanoruler: Principle and applications. *Journal of Photochemistry and Photobiology C: Photochemistry Reviews* **12**:1, 20-30 (2011).

[5] (ed.): *Instrument Society of America: Electrical Transducer Nomenclature and Terminology "Standard MC6. 1-1975 (R1982)."*,

[6] W. Göpel; (ed.): *Sensors: a Comprehensive Survey Chemical and Biochemical Sensors Part I* New York, VCH Publishers Inc. 1991.

[7] W. Göpel; T. Grandke (ed.): *Sensors: a Comprehensive Survey Fundamentals and General Aspects* New York, VCH Publishers Inc. 1989.

[8] S. Middelhoek; D. J. W. Noorlag: Signal conversion in solid-state transducers. *Sensors and Actuators* **2**:211-228 (1981).

[9] International Vocabulary of Metrology – Basic and General Concepts and Associated Terms (VIM 3rd edition) JCGM 200:2012.

[10] W. Göpel; E. Wagner (ed.): *Sensors: a Comprehensive Survey Optical Sensors*. New York, VCH Publishers Inc. 1992.

[11] N. I. Georgiev, et al.: A novel water-soluble 1,8-naphthalimide as a fluorescent pH-probe and a molecular logic circuit. *Journal of Luminescence* **187**:383-391 (2017).

[12] L. Basabe-Desmonts, et al.: Design of fluorescent materials for chemical sensing. *Chemical Society Reviews* **36**:6, 993-1017 (2007).

[13] J. Wu, et al.: New sensing mechanisms for design of fluorescent chemosensors emerging in recent years. *Chemical Society Reviews* **40**:7, 3483-3495 (2011).

[14] S. L. Wiskur, et al.: Teaching Old Indicators New Tricks. *Accounts of Chemical Research* **34**:12, 963-972 (2001).

[15] A. P. de Silva, et al.: Fluorescent PET (Photoinduced Electron Transfer) sensors as potent analytical tools. *Analyst* **134**:12, 2385-2393 (2009).

[16] H. S. Jung, et al.: Fluorescent and colorimetric sensors for the detection of humidity or water content. *Chemical Society Reviews* **45**:5, 1242-1256 (2016).

[17] A. P. de Silva, et al.: Signaling Recognition Events with Fluorescent Sensors and Switches. *Chemical Reviews* **97**:5, 1515-1566 (1997).

[18] J. Zhao, et al.: Excited state intramolecular proton transfer (ESIPT): from principal photophysics to the development of new chromophores and applications in fluorescent molecular probes and luminescent materials. *Physical Chemistry Chemical Physics* **14**:25, 8803-8817 (2012).

[19] X. Zhou, et al.: Recent Progress on the Development of Chemosensors for Gases. *Chemical Reviews* **115**:15, 7944-8000 (2015).

[20] S. Haremsa: *Naphthalimide Dyes and Pigments.* Ullmann's Encyclopedia of Industrial Chemistry Weinheim, Germany, W.-V. V. G. Co. 2000.

[21] Y. Fu, et al.: A novel 1,8-naphthalimide derivative as an efficient silver(I) fluorescent sensor. *Journal of Luminescence* **178**:156-162 (2016).

[22] A. T. Peters; M. J. Bide: Amino derivatives of 1,8-naphthalic anhydride and derived dyes for synthetic-polymer fibres. *Dyes and Pigments* **6**:5, 349-375 (1985).

[23] M. Cao, et al.: Naphthalimide-based fluorescent probe for selectively and specifically detecting glutathione in the lysosomes of living cells. *Chemical Communications* **52**:4, 721-724 (2016).

[24] X. Li, et al.: The novel anti-tumor agents of 4-triazol-1,8-naphthalimides: Synthesis, cytotoxicity, DNA intercalation and photocleavage. *European Journal of Medicinal Chemistry* **46**:4, 1274-1279 (2011).

[25] R. Shen, et al.: A sensitive fluorescent probe for cysteine and Cu2+ based on 1,8-naphthalimide derivatives and its application in living cells imaging. *Tetrahedron* **73**:4, 373-377 (2017).

[26] L. Jia, et al.: A novel chromatism switcher with double receptors selectively for Ag+ in neutral aqueous solution: 4,5-diaminoalkeneamino-N-alkyl-l,8-naphthalimides. *Tetrahedron Letters* **45**:20, 3969-3973 (2004).

[27] Z. Zhang, et al.: A new 1,8-naphthalimide-based colorimetric and “turn-on” fluorescent Hg^{2+} sensor. *Spectrochimica Acta Part A: Molecular and Biomolecular Spectroscopy* **105**:8-13 (2013).

[28] M. Yu, et al.: A 1,8-naphthalimide-based chemosensor with an off-on fluorescence and lifetime imaging response for intracellular Cr3+ and further for S2−. *Dyes and Pigments* **126**:279-285 (2016).

[29] G. Feng, et al.: Fluorogenic and chromogenic detection of biologically important fluoride anion with schiff-bases containing 4-amino-1,8-naphthalimide unit. *Journal of Luminescence* **167**:65-70 (2015).

[30] M. Yu, et al.: A novel colorimetric and fluorescent probe for detecting fluoride anions: from water and toothpaste samples. *Tetrahedron* **72**:2, 273-278 (2016).

[31] Y.-K. La, et al.: A 1,8-naphthalimide-based chemosensor for dual-mode sensing: colorimetric and fluorometric detection of multiple analytes. *RSC Advances* **6**:87, 84098-84105 (2016).

[32] L. Dai, et al.: A naphthalimide-based fluorescent sensor for halogenated solvents. *Chemical Communications* **52**:10, 2095-2098 (2016).

[33] J. Szejtli: Introduction and General Overview of Cyclodextrin Chemistry. *Chemical Reviews* **98**:5, 1743-1754 (1998).

[34] A. R. Hedges: Industrial Applications of Cyclodextrins. *Chemical Reviews* **98**:5, 2035-2044 (1998).

[35] T. Korpela, et al.: Cyclodextrins: Production, properties and applications in food chemistry. *Food Biotechnology* **2**:2, 199-210 (1988).

[36] G. Crini: Review: A History of Cyclodextrins. *Chemical Reviews* **114**:21, 10940-10975 (2014).

[37] T. Loftsson; M. E. Brewster: Pharmaceutical applications of cyclodextrins: basic science and product development. *Journal of Pharmacy and Pharmacology* **62**:11, 1607-1621 (2010).

[38] S. Li; W. C. Purdy: Cyclodextrins and their applications in analytical chemistry. *Chemical Reviews* **92**:6, 1457-1470 (1992).

[39] W. Saenger: Cyclodextrin Inclusion Compounds in Research and Industry. *Angewandte Chemie International Edition in English* **19**:5, 344-362 (1980).

[40] A. Ueno: Review: fluorescent cyclodextrins for molecule sensing. *Supramolecular Science* **3**:1, 31-36 (1996).

[41] M. Fumio, et al.: Excimer Formation and Induced-Fit Type of Complexation of β-Cyclodextrin Capped by Two Naphthyl Moieties. *Bulletin of the Chemical Society of Japan* **60**:10, 3619-3623 (1987).

[42] K. Hamasaki, et al.: Fluorescent sensors of molecular recognition. Modified cyclodextrins capable of exhibiting guest-responsive twisted intramolecular charge transfer fluorescence. *Journal of the American Chemical Society* **115**:12, 5035-5040 (1993).

[43] A. Ueno, et al.: Association, photodimerization, and induced-fit types of host-guest complexation of anthracene-appended .gamma.-cyclodextrin derivatives. *Journal of the American Chemical Society* **110**:13, 4323-4328 (1988).

[44] Y. Liu, et al.: Novel Permethylated β-Cyclodextrin Derivatives Appended with Chromophores as Efficient Fluorescent Sensors for the Molecular Recognition of Bile Salts. *The Journal of Organic Chemistry* **72**:22, 8227-8234 (2007).

[45] H. Ikeda, et al.: Skeleton-selective fluorescent chemosensor based on cyclodextrin bearing a 4-amino-7-nitrobenz-2-oxa-1,3-diazole moiety. *Organic & Biomolecular Chemistry* **3**:23, 4262-4267 (2005).

[46] J. Wu, et al.: Chromogenic/Fluorogenic Ensemble Chemosensing Systems. *Chemical Reviews* **115**:15, 7893-7943 (2015).

[47] T. Muhammad Nazir, et al.: A Rapid Click Chemistry Using Beta-Cyclodextrin Immobilized on Glass Micro-Particles. *Letters in Organic Chemistry* **10**:4, 269-276 (2013).

[48] X. D. Liu, et al.: Surface modification of nonporous glass beads with chitosan and their adsorption property for transition metal ions. *Carbohydrate Polymers* **49**:2, 103-108 (2002).

[49] H. Zengin, et al.: Glass bead grafting with poly(carboxylic acid) polymers and maleic anhydride copolymers. *Polymers for Advanced Technologies* **19**:2, 105-113 (2008).

[50] J. Y. Li; S. Nemat-Nasser: Micromechanical analysis of ionic clustering in Nafion perfluorinated membrane. *Mechanics of Materials* **32**:5, 303-314 (2000).

[51] J. Peron, et al.: Properties of Nafion® NR-211 membranes for PEMFCs. *Journal of Membrane Science* **356**:1, 44-51 (2010).

[52] M. A. Hickner, et al.: Alternative Polymer Systems for Proton Exchange Membranes (PEMs). *Chemical Reviews* **104**:10, 4587-4612 (2004).

[53] K. A. Mauritz; R. B. Moore: State of Understanding of Nafion. *Chemical Reviews* **104**:10, 4535-4586 (2004).

[54] S. Litster; G. McLean: PEM fuel cell electrodes. *Journal of Power Sources* **130**:1, 61-76 (2004).

[55] C. Heitner-Wirguin: Recent advances in perfluorinated ionomer membranes: structure, properties and applications. *Journal of Membrane Science* 120:1, 1-33 (1996).

[56] G. Gelbard: Organic Synthesis by Catalysis with Ion-Exchange Resins. *Industrial & Engineering Chemistry Research* **44**:23, 8468-8498 (2005).

[57] A. Yasuda; T. Shimidzu: Electrochemical carbon monoxide sensor with a Nafion® film. *Reactive and Functional Polymers* **41**:1, 235-243 (1999).

[58] Z. Zheng, et al.: Highly sensitive amperometric Pt–Nafion gas phase nitric oxide sensor: Performance and application in characterizing nitric oxide-releasing biomaterials. *Analytica Chimica Acta* **887**:186-191 (2015).

[59] J. E. Madden, et al.: Nafion-based optode for the detection of metal ions in flow analysis. *Analytica Chimica Acta* **319**:1, 129-134 (1996).

[60] T. J. Sands, et al.: A highly versatile stable optical sensor based on 4-decyloxy-2-(2-pyridylazo)-1-naphthol in Nafion for the determination of copper. *Sensors and Actuators B: Chemical* **85**:1, 33-41 (2002).

[61] C.-M. Chan; K.-Y. Wong: Evaluation of a luminescent ruthenium complex immobilized inside Nafion as optical pH sensor. *Analyst* 123:9, 1843-1847 (1998).

[62] P. Iodice, et al.: Ethanol in gasoline fuel blends: Effect on fuel consumption and engine out emissions of SI engines in cold operating conditions. *Applied Thermal Engineering* **130**:1081-1089 (2018).

[63] *ASTM D5501-12(2016), Standard Test Method for Determination of Ethanol and Methanol Content in Fuels Containing Greater than 20% Ethanol by Gas Chromatography, ASTM International, West Conshohocken, PA, 2016*

[64] S. Corsetti, et al.: Characterization of gasoline/ethanol blends by infrared and excess infrared spectroscopy. *Fuel* **141**:136-142 (2015).

[65] L. M. Avila, et al.: Determination of ethanol in gasoline by high-performance liquid chromatography. *Fuel* **212**:236-239 (2018).

[66] F. M. Fortunato, et al.: Expanding the potentialities of standard dilution analysis: Determination of ethanol in gasoline by Raman spectroscopy. *Microchemical Journal* **133**:76-80 (2017).
[67] A. Turanov; A. K. Khitrin: Proton NMR characterization of gasoline–ethanol blends. *Fuel* **137**:335-338 (2014).
[68] P. F. Pereira, et al.: Simultaneous determination of ethanol and methanol in fuel ethanol using cyclic voltammetry. *Fuel* **103**:725-729 (2013).
[69] P. F. Pereira, et al.: Fast batch injection analysis system for on-site determination of ethanol in gasohol and fuel ethanol. *Talanta* **90**:99-102 (2012).
[70] V. Garbarova: Synthesis of supramolecular components with positive charges and study of their binding to plasma treated surfaces. 33-34 (2017)
[71] M. Ozmen, et al.: Surface modification of glass beads with glutaraldehyde: Characterization and their adsorption property for metal ions. *Journal of Hazardous Materials* **171**:1, 594-600 (2009).